

Simulation of Thermal Transport in a Nanocomposite Blow Mold

A thesis presented to
the faculty of
the Russ College of Engineering and Technology of Ohio University

In partial fulfillment
of the requirements for the degree
Master of Science

Deepak Garg

November 2009

© 2009 Deepak Garg. All Rights Reserved.

This thesis titled
Simulation of Thermal Transport in a Nanocomposite Blow Mold

by
DEEPAK GARG

has been approved for
the Department of Mechanical Engineering
and the Russ College of Engineering and Technology by

Khairul Alam
Moss Professor of Mechanical Engineering

Dennis Irwin
Dean, Russ College of Engineering and Technology

ABSTRACT

GARG, DEEPAK, M.S., November 2009, Mechanical Engineering

Simulation of Thermal Transport in a Nanocomposite Blow Mold (99 pp.)

Director of Thesis: Khairul Alam

The thermal design of a nanocomposite mold for the blow molding process has been studied. For low production cycles, there is a significant interest in using lower cost composite molds to replace the expensive traditional metal molds used in the blow molding process. A critical issue in using a polymer matrix composite as an alternative to a metal for mold material is the large difference in the thermal transport properties. The composite mold design must integrate enhanced cooling so that the product can cool sufficiently within a short cycle time. Nanocomposites that use carbon nanofiber offer improvements in thermal and mechanical properties; therefore they are potential candidates for making molds for polymer products. This project describes the design of a nanocomposite blow mold using numerical simulations of the thermal transport in the mold and the stress analysis of the final blow molded product.

Keywords: Blow Mold, Nanocomposite, Polymer processing, Viscoelastic flow, Thermal design.

Approved: _____

Khairul Alam

Moss Professor of Mechanical Engineering

ACKNOWLEDGMENTS

I would like to express my gratitude to everyone who contributed, in different ways, to this project. Inevitably, some names will be missed here.

I would like to express my gratitude and special thanks towards Prof. Khairul Alam, my project supervisor, and Dr. Hajrudin Pasic for their advice, support and patience. At every crucial point of my project, they have always been there to guide and encourage me.

I would also like to thank Dr. Peter Klein and Dr. John Deno, Department of Industrial Technology, for their suggestions and assistance during the project. I am also thankful to Dr. Calin Druma and Jason Morosko for their help during the project.

I am also thankful to Mr. Vivek Kumar from POLYFLOW technical support for his help with the POLYFLOW model. I would also like to thank Mr. John Perdikoulias from Accuform, Canada to help me with the B-SIM simulations.

Last but not the least I would like to thank the mechanical engineering department and the Partners in Plastics for providing me with the opportunity to have such a great learning experience.

TABLE OF CONTENTS

	Page
Abstract.....	3
Acknowledgments.....	4
List of Figures.....	9
Chapter 1: Introduction.....	12
1.1: Blow Molding.....	12
1.2: Quality of Final Blow Molded Product.....	15
1.3: Mold Material.....	16
1.4: Need of Alternate Materials and Nanocomposites.....	17
1.5: Objective.....	18
Chapter 2: Composites.....	20
2.1: Carbon Composites and Nanocomposites.....	20
2.2: Types of Nanocomposites.....	21
2.3: Properties of Nanocomposites.....	21
2.4: Nanocomposites as Mold Material.....	24
Chapter 3: Design of Blow Mold.....	26
3.1: Mold Material.....	27
3.2: Manufacturing of Nanocomposite Mold Core.....	29
3.3: Design of Cooling System.....	32
Chapter 4: Temperature Analysis using ALGOR.....	35
4.1: Solid Edge Model.....	35

	6
4.2: ALGOR Model	35
4.3: Design of Cooling System using ALGOR.....	40
4.4: Summary of Thermal Simulations.....	50
Chapter 5: Manufacturing of Nanocomposite Blow Mold	54
Chapter 6: Stress Analysis in POLYFLOW	60
6.1: Solid Edge Model	60
6.2: Gambit Meshing	61
6.3 Parison Thickness	62
6.3.1: Tracking of Material Movement.....	62
6.4: Material Properties for POLYFLOW Model.....	64
6.5: Boundary Conditions	65
6.5.1: Flow Boundary Conditions.....	65
6.5.2: Thermal Boundary Conditions	67
6.6: Remeshing	68
6.7: POLYFLOW Models.....	70
6.7.1: Function for Viscosity	71
6.8: Stress Postprocessor.....	74
6.8.1: Newtonian Models.....	74
(a) Isothermal Flow Problem with Constant Viscosity.....	75
(b) Generalized Newtonian Isothermal Flow Problem	78
(c) Generalized Newtonian Non-isothermal Flow Problem	82
6.8.2: Integral Viscoelastic Models	85

	7
(a) KBKZ Shell Model (2-D Model)	88
(b) Non-isothermal KBKZ Shell Model (3-D)	89
Chapter 7: B-SIM Model	90
Chapter 8: Discussion and conclusions.....	94
Chapter 10: Future Work	96
References.....	98

List of Tables

	Page
Table 1: Material properties used for ALGOR simulations.....	36
Table 2: Boundary conditions for the ALGOR simulations	40
Table 3: Different designs of cooling channels	50
Table 4: Material properties common to all POLYFLOW models	65
Table 5: Contact problem parameters	67
Table 6: Remeshing settings for Lagrangian and Thompson remeshing techniques.....	69
Table 7: Parameters for modified Cross law.....	74
Table 8: Eight node spectrum of partial viscosities and relaxation times.....	87

LIST OF FIGURES

	Page
Figure 1(a): Schematic of extrusion blow molding with the required equipment	14
Figure 1(b): Schematic of extrusion blow molding for a plastic wheel showing the extruder, the parison and the two mold halves	14
Figure 2: Variation of thermal conductivity of carbon/carbon composites and nanocomposites with heat treatment temperature	23
Figure 3: Variation of deflection in thickness direction with increase in mold thermal conductivity	25
Figure 4: Mold used for manufacturing of wheels	26
Figure 5: SEM picture of the nanocomposite mold material	28
Figure 6: Manufacturing of nanocomposite mold by using a plug inside metal fixture	30
Figure 7: Heating and pressing of mold core in the metal fixture	31
Figure 8: Nanocomposite mold core after removal from the metal fixture	31
Figure 9: Dimensions of the mold core	32
Figure 10: Solid edge model of the mold with polymer layer in the shape of the fully blown wheel	35
Figure 11: ALGOR meshed model of the mold with polymer layer	37
Figure 12: Temperature profile for design 1	41
Figure 13: Temperature profile for design 2	42
Figure 14: Temperature profile for design 3	43
Figure 15: Temperature profile for design 4	44

Figure 16: Temperature profile for design 5.....	45
Figure 17: Temperature profile for design 6.....	46
Figure 18: Temperature profile for design 7.....	47
Figure 19: Temperature profile for design 8.....	48
Figure 20: Temperature profile for design 9.....	49
Figure 21: Variation of maximum temperature at the end of the cycle during steady cyclic state with increase in convection coefficient on the inner surface.....	52
Figure 22: Maximum temperature vs time during a cycle for design no. 7.....	53
Figure 23: Orthographic views of the blow mold for final machining.....	55
Figure 24: Isometric view of the blow mold core for final machining.....	56
Figure 25: Nanocomposite mold core with cooling channels and groves at two sides for gripping the mold structure.....	56
Figure 26: Mold half with nanocomposite mold core.....	57
Figure 27: Mold half with flat surface.....	58
Figure 28: Mold halves held by guide pins.....	59
Figure 29: Solid Edge model for mold along with the parison.....	60
Figure 30: Meshed model in Gambit.....	61
Figure 31: Tracking of material points at different times during a blow cycle.....	63
Figure 32: Parison dimensions.....	64
Figure 33: Parison boundaries.....	66
Figure 34: Global coordinates for parison remeshing.....	70
Figure 35: Variation of shear rate for constant viscosity model.....	72

Figure 36: Variation of σ_1 for Newtonian model with constant viscosity	76
Figure 37: Variation of σ_2 for Newtonian model with constant viscosity	77
Figure 38: Variation of σ_3 for Newtonian model with constant viscosity	77
Figure 39: Variation of shear rate for Newtonian isothermal model with variable viscosity	79
Figure 40: Variation of σ_1 for Newtonian isothermal model with variable viscosity.....	80
Figure 41: Variation of σ_2 for Newtonian isothermal model with variable viscosity.....	81
Figure 42: Variation of σ_3 for Newtonian isothermal model with variable viscosity.....	81
Figure 43: Variation of shear rate for Newtonian non-isothermal model with variable viscosity	82
Figure 44: Variation of σ_1 for Newtonian non-isothermal model with variable viscosity	83
Figure 45: Variation of σ_2 for Newtonian non-isothermal model with variable viscosity	84
Figure 46: Variation of σ_3 for Newtonian non-isothermal model with variable viscosity	84
Figure 47: Meshed model – 2D KBKZ model.....	89
Figure 48: Stages of expanding parison in B-SIM simulation.....	91
Figure 49: Thickness profile in the blow molded wheel.....	92
Figure 50: Von-Mises stress profile in the final blow molded wheel.....	93

CHAPTER 1: INTRODUCTION

1.1: Blow Molding

Blow molding is one of the most popular manufacturing processes used for production of hollow plastic parts. This process is used to make hollow parts from thermoplastic materials. It is mainly used to manufacture parts with reentrant curves which are otherwise not possible with injection molding. Blow molding is also less expensive than injection molding. The operating pressures for blow molding vary from 25 psi to 150 psi whereas injection molding incorporates pressures from 2000 to 20000 psi. The low operating pressures for blow molding leads to lower internal stresses in the final product which makes this a good alternative for many products (Rosato et al., 2004).

There are very few publications that describe the blow molding process. The following description in this chapter is primarily summarized from the blow molding handbook by D. V. Rosato, A. V. Rosato & D. P. Dimattia. Blow molding can be categorized into two main categories: Extrusion blow molding and Injection blow molding. In extrusion blow molding, resin and plastic pellets are melted to form a homogeneous mixture which is then extruded to form a parison. The parison is not supported on any core. But in injection blow molding, the preform is injection molded over a metal core. There is also a third type of blow molding, i.e. stretch blow molding but it starts with either injection blow molding or extrusion blow molding. The choice of the blow molding process depends on the final product, raw material, cost of production and quantity (Rosato et al., 2004).

Extrusion blow molding is advantageous for large production volume. It uses low cost tools and there is a wide variety of machine vendors available for extrusion blow molding machine parts. But extrusion blow molding has a high scrap rate and it does not offer any control on the thickness of the final product. Trimming is required for the final product. Injection blow molding produces very little scrap or none at all and it is much more controlled as compared to extrusion blow molding. But injection blow molding uses high cost tools and it is only used for low production volumes. So there has to be a tradeoff while choosing the blow molding process (Rosato et al., 2004).

In the present analysis, extrusion blow molding is studied for the possibility of an alternative mold material. In extrusion blow molding, the polymer material is first melted and made into a tube, which is called a parison. This parison tube is closed at one end. The parison is held in the mold and pressurized air is then blown into the tube. The pressure expands the parison tube to the shape of the cavity. The tube forms a layer on the inner walls of the cavity, and high pressure is maintained till the soft polymer layer has cooled down and solidified. Then the pressure is released and the solid part is ejected from the mold and a fresh parison tube is put inside the mold cavity for the next part. The schematic of the blow molding setup can be seen in Figure 1(a) and (b). Figure 1(a) shows the blow molding process equipment, and Figure 1(b) shows the blow mold for a plastic wheel along with the parison. The time taken to manufacture a part is called the cycle time.

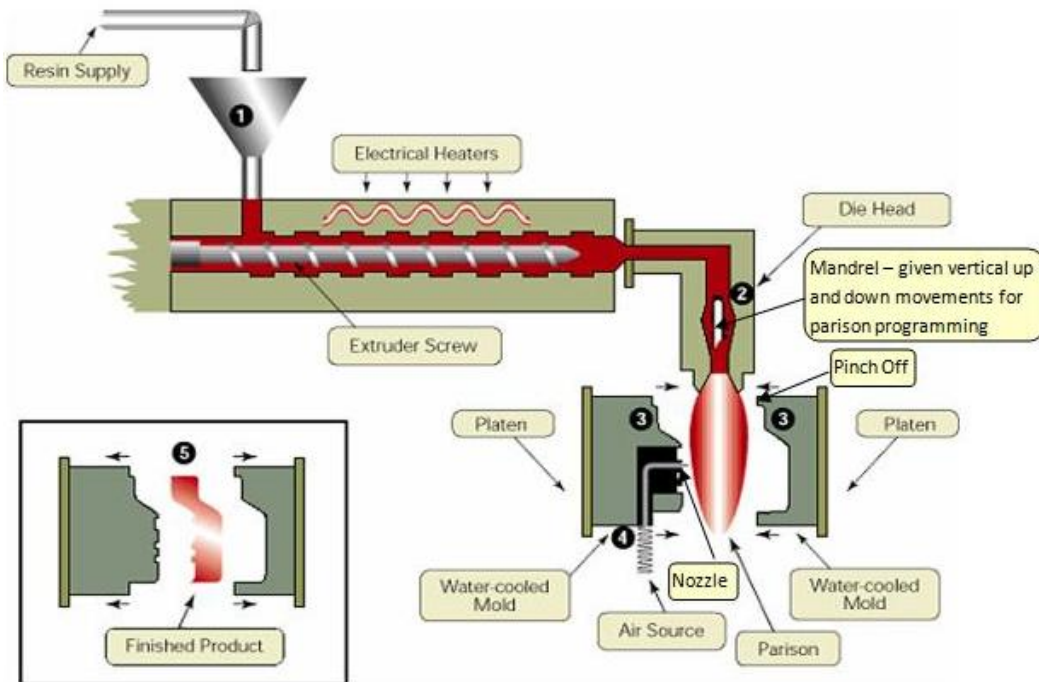


Figure 1(a): Schematic of extrusion blow molding with the required equipment (Strong, 2008)

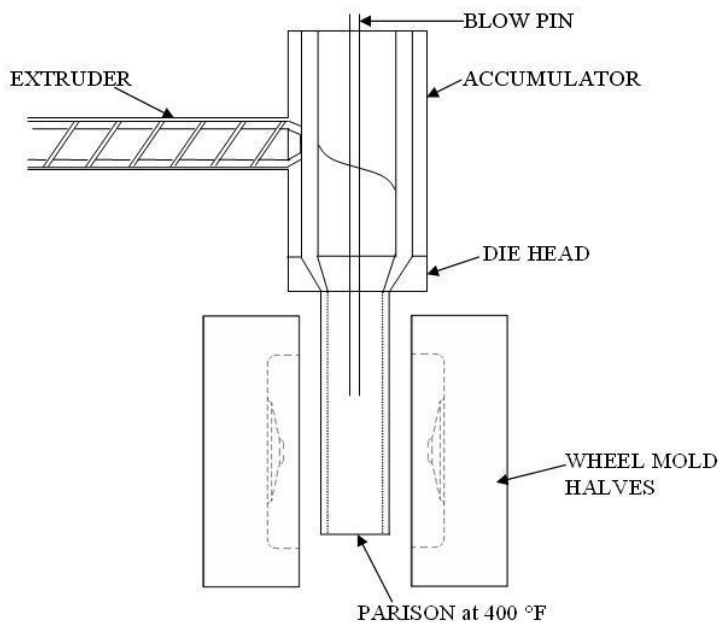


Figure 1(b): Schematic of extrusion blow molding for a plastic wheel showing the extruder, the parison and the two mold halves (Engineer's Handbook, 2006; Alam et al., 2009)

1.2: Quality of Final Blow Molded Product

The quality of the final product is mainly controlled by the properties of the raw material and polymer-resin melt. As the density and crystalline nature of the raw material increases, the rigidity of final part increases. Increase in density of the raw material produces abrasion resistant and permeation resistant final products. However, the stress cracks due to residual stresses increase with increase in density. As the melt index of the raw material increases, the flow rate will increase. This leads to a decrease in the heat input by the extruder. The sagging of the parison by its own weight puts an upper limit on the melt index of the raw material to be used (Rosato et al., 2004).

Air is introduced into the parison mainly through the mandrel of the extruder, through the blow pin over which the parison drops or through the needles which pierce the parison. Extrusion blow molding does not have any direct control over the thickness of the part. The thickness is controlled by controlling the thickness of the parison. This process is called as parison programming. The mandrel is given vertical movements to vary the thickness of the extruding parison along its length so that the final product can have thicknesses only within a certain range.

The quality of the product also depends on the design of blow mold and process of solidification. Mold cavity should have some vents to remove any air trapped between the parison and the cavity surface. There must be a good contact between the blown parison and the cavity surface. Corners of a blow mold are the last places to be filled by the blown parison so the expanding parison will push the entrapped air towards these corners. Therefore corners of a blow mold should be well vented. Otherwise the final

product will not have sharp finished corners. A smooth surface of the cavity is preferred; so there is an upper limit to ventilation control otherwise it will result in a blown product with a rough surface, which is not desirable (Rosato et al., 2004).

The air trapped between the parison and mold cavity also inhibits the cooling of the blown parison. So venting helps in decreasing the cycle time for the product. The blow molded part should be cooled in a controlled way to minimize any post-cooling problems like shrinkage and warping. The temperature variations along the final blow molded part should be minimized. These temperature variations along the ejected part may cause deformations in the final product. The product should be cooled down uniformly as much as possible.

The cooling technique also has an affect on the thickness variations in the final product. If the temperature in the pinch off area is too low, then the parison will not expand in that portion. This results in thicker walls near pinch off areas and thinner walls at the ends. And if the temperature is too high, it will result in thinner walls near pinch off area and thicker walls at the ends (Rosato et al., 2004).

1.3: Mold Material

The rate of production depends on the cycle time, which depends on the rate at which the thin polymer layer solidifies. For a faster rate of solidification, the mold material should have high thermal conductivity. The mold material should be chosen such that it maintains its dimensional accuracy after cyclic thermal loads and at processing temperatures. The mold material should have enough strength, stiffness and hardness. Because of all these reasons, specific metals (aluminum) and alloys (hardened

steel, pre-hardened steel, beryllium-copper alloy) are selected for blow mold material. The mold cost is a major part of the total manufacturing cost. But the cost of the material is not the only factor of concern while choosing a mold material. It also depends on the life span of the mold. In other words, it also depends on the number of parts that can be manufactured without noticeable wear in the mold. In short, the cost of the material, the cost of machining and the number of parts manufactured determine the cost-effectiveness of the mold material. Metal blow molds have proved to be cheaper for higher production volumes (10^7 parts per mold). The cost of the product increases if the mold is used for smaller production volumes.

1.4: Need of Alternate Materials and Nanocomposites

In the current manufacturing environment, the part designs are changing rapidly and so are the molds. It is very expensive to machine a mold out of a solid piece of metal. So the plastics industry is always looking for an alternative material for the molds. Nanocomposite molds may be a viable solution to the problem.

Nanocomposites are manufactured by binding nano size filler with a matrix using a binder. Nanocomposites will be explained in detail in the chapter 2. Nanocomposite molds can be expected to be cheaper, easier to machine and resistant to corrosion. Nanocomposites have the advantages of lower machining cost and quicker turnaround time. Nano-composite molds are much lighter as compared to metal molds which make it easier to transport and support them. But the life span of the nano-composite molds may be much less as compared to metals molds. This makes the nano-composite material a better material for low production volumes.

Several issues must be examined before a polymer matrix composite (such as a nanocomposite) can be adopted for making a blow molding tool. A major issue in the use of the nanocomposite mold is its thermal conductivity, which is much lower than metal molds. The thermal conductivity of a typical polymer is about 0.2 W/mK. This is about two orders of magnitude lower as compared to alloys such as stainless steel. Even if the addition of carbon-nano fibers increases the conductivity of resulting composite to about 2 W/mK, it would still be lower as compared to metal. The lower thermal conductivity of the nanocomposite makes it difficult to cool the polymer part within the desired cycle time and to control the cooling process. Therefore the thermal management problem associated with a blow molding tool can be quite severe for the case of a nanocomposite tool, unless the product is cooled and solidified in a controlled fashion. The cycle time can be very long and undesirable residual stresses can cause loss of dimensional accuracy. This would increase the product cost (Alam et al., 2009).

1.5: Objective

This research aims at the designing and testing of a new type of blow mold made of a nanocomposite material with polymer matrix. The nanocomposite material used in this study is made by University of Dayton Research Institute (UDRI). The mold material has carbon nanotubes as the filler material. The objective of this research is to provide blow molding industry with an alternate mold material other than metals. As already discussed, the thermal conductivity of the nanocomposite is very low ($\approx 2\text{W/mK}$). The primary objective of this study is to design a nanocomposite blow molding tool with emphasis on the thermal processes that take place during molding. This research is

focused on the cooling of the thin polymer layer to a temperature below the specified ejection temperature within a specified cycle time. The mold will be designed on the basis of computer simulations using ALGOR and POLYFLOW softwares.

The thermal simulation parts of the study described in this thesis has already been published (Alam et al., 2009) earlier. In addition to the thermal analysis, this study includes simulation of the wall thickness, final shape and properties of the final product, as predicted on the basis of computer simulations on ALGOR and POLYFLOW. In addition, simulation using a commercial blow molding software (B-SIM) is also discussed.

CHAPTER 2: COMPOSITES

There are three types of basic materials – metals, polymers and ceramics. If two or all of these material types are combined to form a new material, it is called a composite. The advantage of composites lies in combining the materials with entirely different properties. Polymers are light and have good impact strength and can be flexible. Ceramics are good electrical insulators, chemically resistant and have high Young's modulus but they are heavy and brittle. Metals are strong, ductile and good conductors of heat and electricity. Every class of material has its strengths and weaknesses according to particular applications. So mixing of these material types to get composites can provide excellent properties (Fitzer & Manocha, 1998).

2.1: Carbon Composites and Nanocomposites

Carbon composites are manufactured by embedding carbon filler in a matrix which binds the filler. The binder may be a resin such as phenol or pitch. Different type of carbon composites can be made by varying the size of filler, type of filler, matrix or the binder. The typical fillers are carbon flakes, soot or carbon fibers. The carbon composites have wide variety of applications due to their unique mechanical and thermal properties.

Carbon nanocomposite materials are manufactured by combining two or more different materials, such that one or more of the components have at least one dimension in the order of nanometers. Nanocomposite is composed of a continuous matrix and a discontinuous reinforcing phase. These materials can be obtained by introducing nano size fibers in a matrix. The fibers improve the qualities of the matrix material

significantly. For example, when carbon nanotubes are used as filler in a polymer, it adds to electrical and thermal conductivity of the polymer. They also add to the mechanical properties (strength, modulus, dimensional stability, etc.) of the polymer. Traditional composite materials have 30-40 % of the reinforcement material but nanocomposites start to show improvements with reinforcement of mass fraction of as small as 5 % (Fitzer & Manocha, 1998).

2.2: Types of Nanocomposites

Carbon nanotubes based nanocomposites have been classified by Ajayan et al. (1996) into two broad types – extrinsic nanocomposites and intrinsic nanocomposites. In extrinsic nanocomposites, carbon tubes are present in their unmodified form. There is no chemical, physical or structural modification in the carbon nanotubes. The matrix material just wets or fills the carbon nanotubes and act as a binder to keep the composite together. On the other hand, intrinsic nanocomposites have carbon nanotubes modified during or after they are synthesized. The intrinsic nanocomposites can be manufactured by the in-situ modification of carbon nanotubes by introducing foreign elements into the plasma arc discharge (Ajayan et al., 1996).

2.3: Properties of Nanocomposites

The properties of a nanomaterial depend on its structure, which in turn depends on the process by which it is manufactured. Nanomaterials are available in different structures like thin films (semiconductors), layered structures (silicon clays) and 3-D uniform clusters (magnesium oxide) (Ajayan et al., 1996). Carbon nanotubes have become important as a nano material with a variety of applications. The properties of

nanocomposites, like a normal composite, depend on its components and their interface properties. Nanocomposites, with chemically modified nanotubes, can be made to have a wide range of properties by introducing different foreign elements (Ajayan et al., 1996).

The thermal conductivity of carbon nanotubes is measured to be 1800-6000 W/mK at room temperature, which is much higher than that of carbon fibers (600-1100 W/mK). Gong et al. (2004) measured the thermal conductivity of aligned carbon nanotubes/carbon composites. They reported that the thermal conductivity of aligned carbon nanotubes/carbon composites increase with increase in the heat treatment (graphitization) temperature. The variation of thermal conductivity of carbon composites with increase in heat treatment temperature can be seen in Figure 2.

After heat treatment at 3000°C, the thermal conductivity of aligned carbon nanocomposites made by Gong et. al (2004) has been reported to be 72 W/mK. The corresponding thermal conductivity of conventional carbon-carbon composite was reported to be 64 W/mK. But after taking all the factors (thermal diffusivity, fraction of carbon fibers or carbon nanotubes, and density) into consideration, the nanocomposites with aligned carbon nanotubes were reported to be better at thermal conduction as compared to the conventional carbon-carbon composites (Gong et al., 2004).

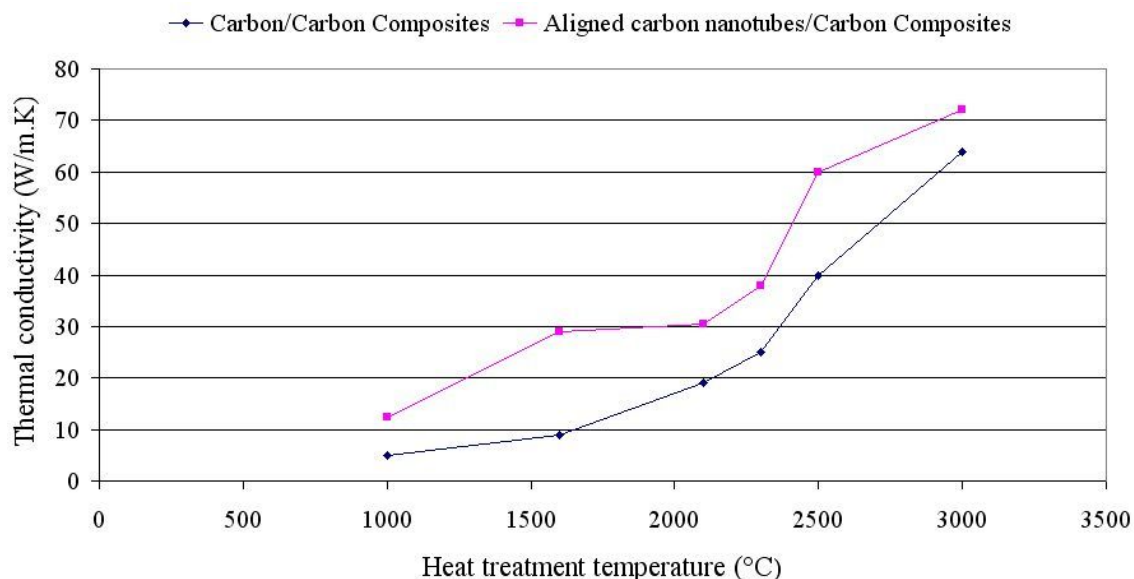


Figure 2: Variation of thermal conductivity of carbon/carbon composites and nanocomposites with heat treatment temperature (Gong et al., 2004)

The axial young modulus of carbon nanotubes is reported to be in the range of 0.45 to 5.0 TPa based on different tests (Gong et al., 2004). But still, most carbon nanofiber composites are not good as compared to convention carbon composites because nanotubes are not well bonded to matrix (Gong et al., 2004). Due to these weak bonds, the overall properties of composites are not good as might have been expected. Nanocomposites with surface modified nanotubes are much stronger as far as the bonding between nanotubes and matrix material is concerned. These nanocomposites have a high strength to weight ratio as compared to metals and conventional carbon composite. It makes these intrinsic nanocomposites a good alternative for structural applications (Gong et al., 2005).

2.4: Nanocomposites as Mold Material

Although very few studies exist on the use of nanocomposite to replace a metal mold, a recent publication by Han and Rice (2008) describes the use of this nanocomposite material for making an injection mold. This work is summarized below.

A nanocomposite mold was compared by Han and Rice (2008) to a metal mold for strength and heat transfer capability. The nanocomposite mold was found to be incapable of doing the required heat transfer in the cycle time used by metal mold. So the cycle time for nanocomposite mold had to be increased. They also studied the effect of thermal conductivity of the mold material on the warping (part deflection) of the final product. At the end of the cycle, it was observed that the temperature in the metal mold was uniform and the temperature in the nano composite mold was non uniform. It resulted into warping of the final product. The warping of final product decreases with increase in the thermal conductivity of the mold material. The Figure 3 shows the relationship between thermal conductivity of the mold and deflection in the final product.

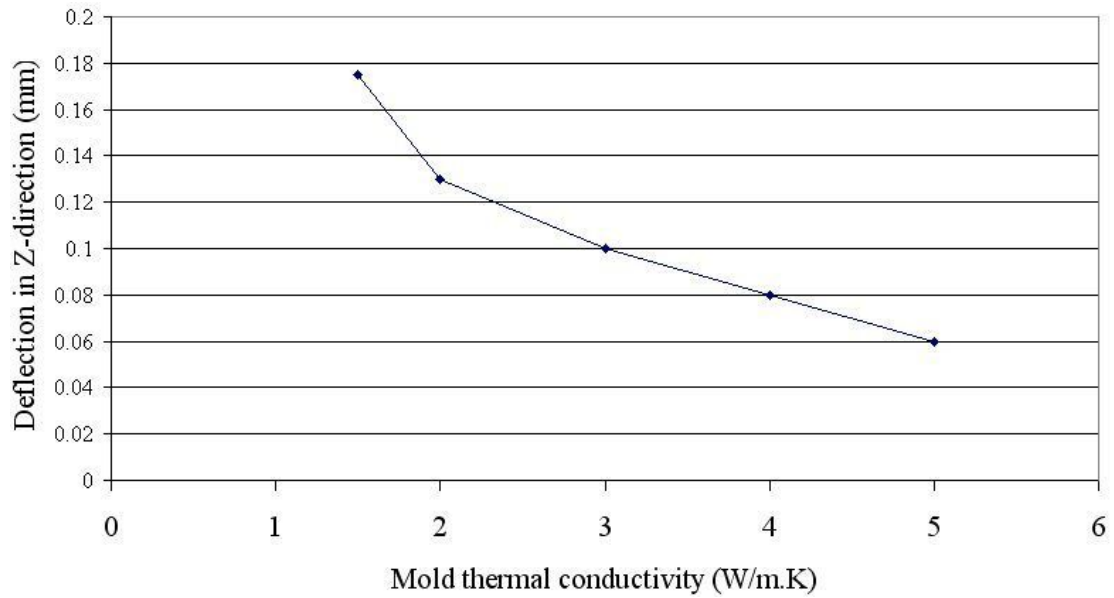


Figure 3: Variation of deflection in thickness direction with increase in mold thermal conductivity (Han & Rice, 2008)

The stress and strain distribution for the nanocomposite mold was also studied.

CHAPTER 3: DESIGN OF BLOW MOLD

The mold is the most important component of the blow molding process. The mold must be an efficient heat sink for the cooling of blow molded products. A blow mold consists of cavity, flash pockets, backing plates, pinch offs, guide pins, cooling channels and vents. A blow mold is usually centrally aligned with the parison but there can be an offset in some special cases (Rosato et al., 2004).

Polymer wheels for toys, small carts, etc., are often manufactured by blow molding. The blow mold used for manufacturing of wheels is typically made out of aluminum. A mold used for manufacturing of a plastic wheel is shown in Figure 4. High density polyethylene (HDPE) is one of the typical polymers used for the manufacturing of these toy wheels. The hot parison is inserted into the mold at about 400 °F (204 °C). The ejection temperature is below 130 °C. The cycle time used for manufacturing is typically about 20 seconds which works well because aluminum is an excellent thermal conductor. So polymer part is cooled quickly below the ejection temperature in the specified cycle time. The aluminum mold is cooled by water circulating through cooling channels. Because of the high conductivity of metals, the placement of cooling channels in a metal mold is not a critical factor; the same is not true of the nanocomposite material (Alam et al., 2009).

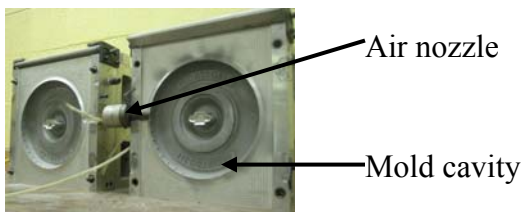


Figure 4: Mold used for manufacturing of wheels (Source: Partners in Plastics, Ohio)

3.1: Mold Material

The choice of materials for a blow mold depends on the number of products that have to be manufactured. Only metals can be used to make blow molds for continuous large scale production. The life span of a steel blow mold is found to be at least 10^7 parts per mold (Rosato et al., 2004). Manufacturing cost of a metal blow mold is generally high because of high machining costs. Aluminum, beryllium-copper and kirksite are typically used for the manufacturing of blow molds.

Blow mold materials typically have the following characteristics (Rosato et al., 2004):

1. Wear resistance against cyclic loads
2. Toughness
3. High modulus
4. High thermal conductivity
5. Machinability for easy manufacturing

The mold material which is used in this research was developed at University of Dayton research institute (UDRI). The mold material is composed of nano fibers, chopped carbon rovings and epoxy. The nano fibers are supplied by ASI (Cedarville, Ohio). The nanocomposite material is mixed together by extruding the components. The extrusion process mixes the components and chops the carbon roving. The result is a “sticky mud” with visible carbon fibers in a matrix of polymer with carbon nano fibers. The epoxy used in the mixture was Epon 862 with Epikure W. It is typically cured for 2 hours at 250°F followed by 2 hours at 350°F at 100psi. The nanocomposite material can be made in the form of continuous sheets of thickness from 80-120 mm and width up to

16 inch. The extruded mixture can also be molded by compression molding. This process is used in making the core of the blow molding tool in this project (Alam et al., 2009).

The properties of the mold material have the benefits of polymer and chopped carbon fibers and carbon nanofibers. Carbon fibers can be seen in the SEM picture, Figure 5. The composite material has a thermal conductivity of 1.653 W/mK in the working temperature range. The density and specific heat of the material are 1440 kg/m³ and 1090 J/kg.K respectively (Han & Rice, 2008).

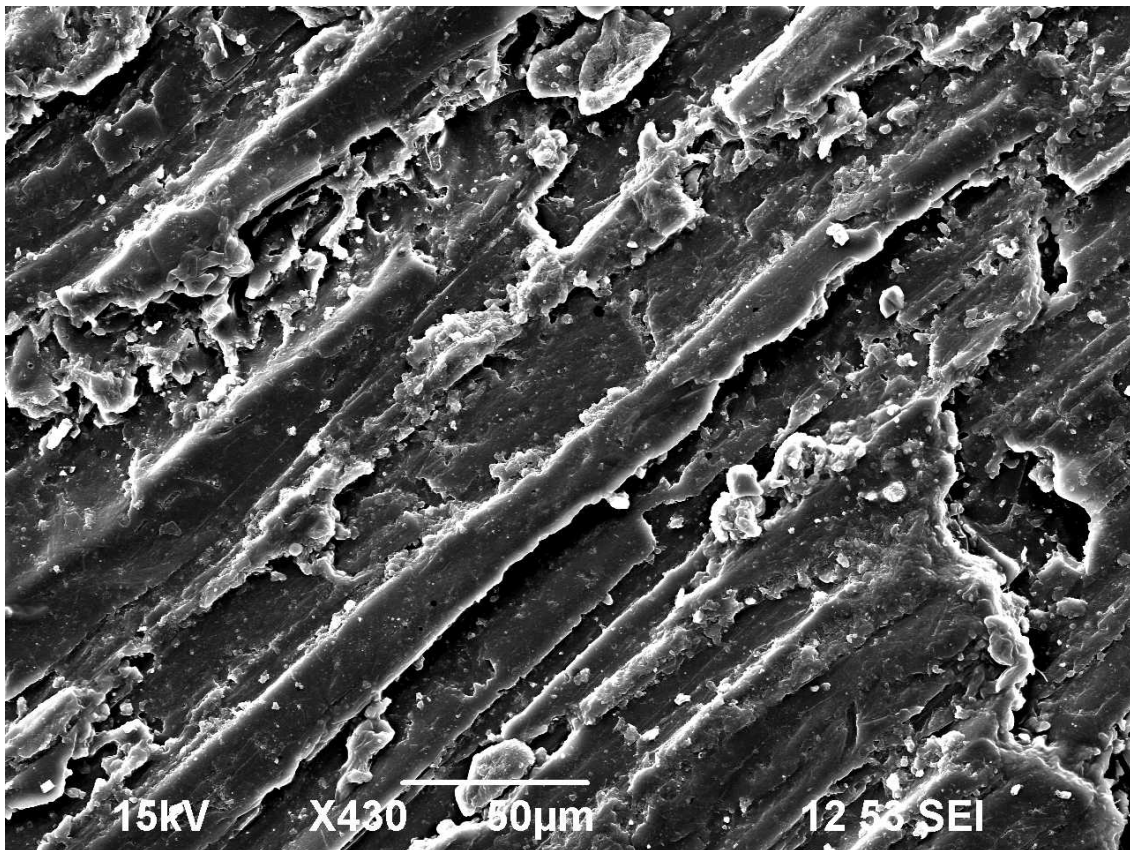


Figure 5: Scanning electron microscope (SEM) picture of the nanocomposite mold material (Source: Center for Advanced Materials Processing (CAMP), Ohio University)

3.2: Manufacturing of Nanocomposite Mold Core

As discussed earlier, all the components (nanofibers, chopped carbon rovings and epoxy) are mixed to form a “sticky mud” like black material. This nanocomposite mixture is molded on a core by compression molding. The mold core was manufactured by UDRI.

The extruded mixture is put into a metal fixture (Figure 6(c)) with an aluminum plug (Figure 6(a)) or wooden plug (Figure 6(b)). However it was determined that compression molding pressures can destroy a wooden plug. So an aluminum plug was used to avoid such problems. After each layer of mold material, a carbon veil (screen) is placed. Once it is packed upto 2.5 inch, the entire assembly was heated and pressed (Figure 7) at the UDRI facility.



(a) Aluminum plug



(b) Wooden plug



(c) Metal fixture with aluminum plug

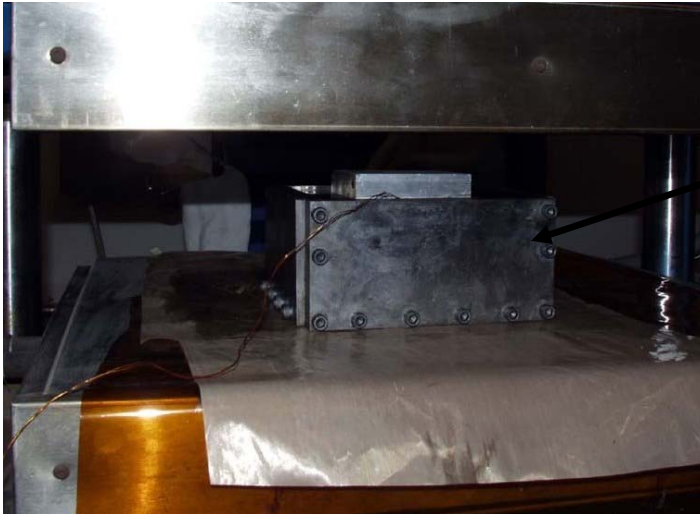


(d) Nanocomposite material in metal fixture



(e) Packed nanocomposite material in the fixture

Figure 6: Manufacturing of nanocomposite mold by using a plug inside metal fixture
(Source: University of Dayton Research Institute (UDRI))



Metal fixture
with composite
core inside

Figure 7: Heating and pressing of mold core in the metal fixture (Source: UDRI)

The nanocomposite mixture on the aluminum plug is slowly heated and compressed to form nanocomposite mold core. Then the mold core is ejected out of the metal fixture (Figure 8).



Raised surface
at center of
wheel

Figure 8: Nanocomposite mold core after removal from the metal fixture (Source: UDRI)

The dimensions of the nanocomposite mold core can be seen in the cutout figure (Figure 9). The cooling channels must be machined in this nanocomposite blow mold before fabrication of full mold.

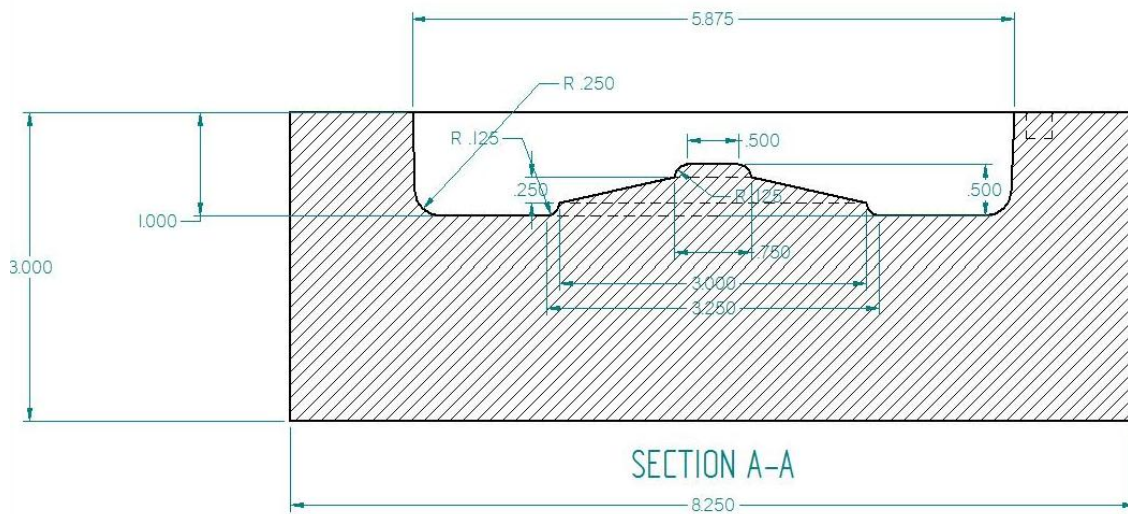


Figure 9: Dimensions of the mold core (All dimensions are in inches)

3.3: Design of Cooling System

Mold cooling takes 80 % of the total cycle time so the design of cooling system is a very critical process for the low cost of the final product. Cooling of the blow molded product can be done in two ways – external cooling and internal cooling.

For external cooling, cooling channels are made around and under the mold cavity and a coolant is passed through these channels. A turbulent flow of the coolant in the external cooling channels is desirable. It will remove more heat as compared to laminar flow. The Reynolds number for the coolant flow should be around 10000 for effective cooling (Rosato et al., 2004).

The Reynolds number increases with the velocity of coolant flow. So for a constant pumping power, the Reynolds number decreases with increase in the radius of cooling channels. Beyond the onset of turbulence, any further increase in the velocity of coolant does not produce significant improvement in the heat transfer.

Internal cooling can be done by using refrigerated air or atomized water or liquid carbon dioxide or liquid nitrogen. The internal coolant is mixed with pressurized air which is used to blow the parison. The coolant vaporizes by gaining heat from the blow molded product and then vaporized coolant is exhausted as a hot gas. It can reduce the blow molding cycle time up to 50%. But internal cooling is not recommended in some cases. It can create strains or spots in the blown parisons (Rosato et al., 2004).

Heat transfer can be enhanced by increasing the diameter of the cooling channels, increasing the flow rate, by using a material with high thermal conductivity, decreasing the distance between the cavity surface and the cooling channels or by lowering the temperature of the coolant. The maximum distance between the cavity surface and the cooling channels depends on the properties of the material and cycle time (Rosato et al., 2004).

The characteristic distance (δ) upto which the cooling effect will travel in a medium in a cycle time of t seconds is of the order of δ (Alam et al., 2009), where

$$\delta = (\alpha t)^{0.5} \quad (1)$$

where α is the diffusivity of the material, and is given by

$$\alpha = K/(\rho C_p) \quad (2)$$

where K is the thermal conductivity

ρ is the density

C_p is the specific heat of the material.

The density, thermal conductivity and specific heat of the nanocomposite mold material are 1.653 W/mK, 1440 kg/m³ and 1090 J/kg.K respectively. So the diffusivity of the mold material, (α):

$$\alpha = K/(\rho C_p) = 1.05 \times 10^{-6} \text{ m}^2/\text{s}.$$

The cycle time is assumed to be 80 seconds. So the characteristic length, δ can be calculated as:

$$\delta = (\alpha t)^{0.5} = 0.36 \text{ inch}.$$

So the surface of cooling tubes should be within a distance of about 0.36 inch from the hot surface of the polymer for sufficient cooling effect (Alam et al., 2009). For this project, the cooling tubes will be designed to be within a distance of quarter inch from surface of the mold cavity.

CHAPTER 4: TEMPERATURE ANALYSIS USING ALGOR

4.1: Solid Edge Model

The solid model of the mold with different designs of cooling tubes is drawn by using Solid Edge software. Due to symmetry, only one-eighth of the mold and product is used in the ALGOR simulations (Figure 10). The final blow molded wheel is assumed of a uniform thickness of 2 mm. A polymer layer of 2 mm can be seen on the top of mold cavity surface in Figure 10. The mold cavity is shown in detail in Figure 9. The cooling tubes are placed around and under the mold cavity.

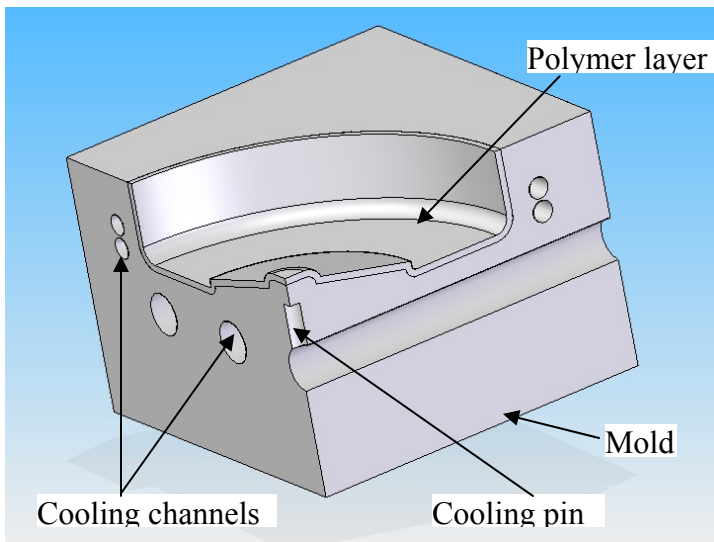


Figure 10: Solid Edge model of the mold with polymer layer in the shape of the wheel

4.2: ALGOR Model

The preliminary transient thermal analysis is performed using ALGOR. Only one eighth of the mold is studied due to symmetry. The problem is modeled as a mold with a 2 mm thick layer of polymer material. The polymer material is chosen as high density

polyethylene (HDPE) from inbuilt ALGOR library. A customized unit system (N, mm, s, K, V, ohm, A, J) is used. The material properties used for ALGOR simulations can be seen in Table 1.

Table 1

Material properties used for ALGOR simulations

Property		Nanocomposite mold	HDPE
Thermal conductivity	W/m.K	1.653	0.3966
	W/mm.K	1.653×10^{-3}	0.3966×10^{-3}
Heat capacity	J/Kg/K	1090	2300
	J/ (N.s ² /mm)/K	1.090×10^6	2.3×10^6
Density	kg/m ³	1440	1382.9
	N.s ² /mm ⁴	1.440×10^{-9}	1.3829×10^{-9}

The model is meshed using automatic meshing with surface mesh size of 50 % fine and solid mesh size of 20 % (as defined in ALGOR). The mold and polymer layer is broken into thermal brick, wedges, pyramids and tetrahedral elements. The total number of nodes and elements in the mold part is 63917 and 83184 respectively. The mold model has 25231 tetrahedral elements, 10014 pyramids, 3415 wedges and 44524 thermal bricks. The polymer layer has 6826 nodes with 5062 elements – 1732 tetrahedral, 934 pyramids, 266 wedges and 2130 thermal bricks. The cycle time for the analysis is assumed to be 80 seconds which gives a characteristic thermal diffusion length of 0.36 inch. The time step

size is 0.5 seconds so that there are 160 steps in 80 seconds (Alam et al., 2009). The meshed model in ALGOR is shown in Figure 11.

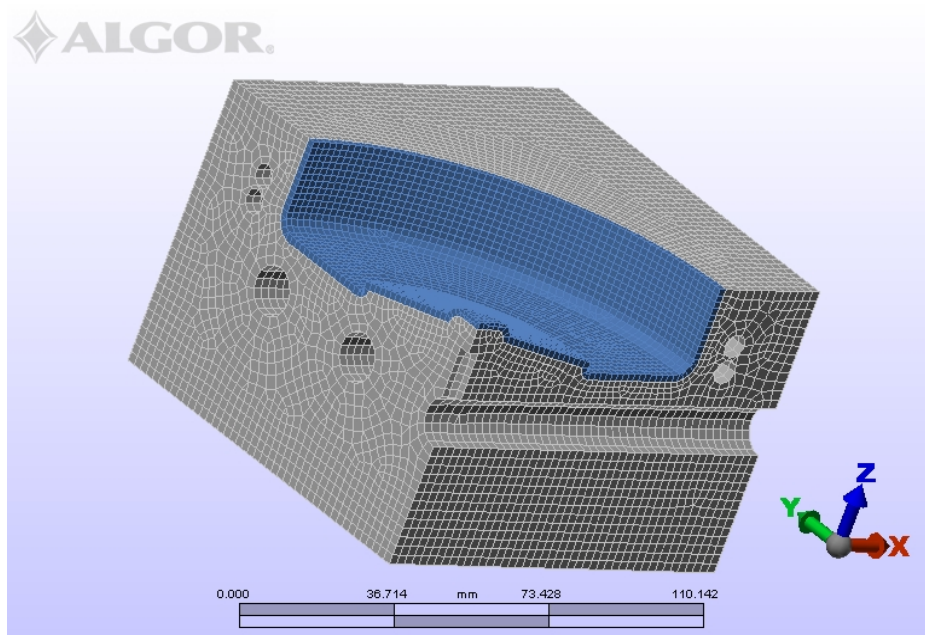


Figure 11: ALGOR meshed model of the mold with polymer layer

To develop the solution for the model, an iterative calculation is used with an initial trial temperature and the trial temperature is updated at the end of the cycle. This process is repeated until convergence, i.e. the history repeats itself each cycle.

The boundary conditions applied on the system are as follows (Alam et al., 2009):

- a) Initial trial temperature of the mold at the starting of first cycle is assumed to be a constant 50°C. The initial temperature of the mold should be chosen carefully. The temperature history of the mold follows a cyclic pattern so the final steady cyclic state temperature of the mold does not depend on the assumed initial

temperature of the mold. But a good assumption of the initial temperature of the mold will make it easier for the model to reach its steady cyclic state quickly.

- b) The initial temperature of the polymer layer is 204°C, which is the temperature at which parison is inserted into the mold.
- c) The surface of the cooling tubes is 10°C which is the temperature of the cooling water. It is assumed that the rate of flow of water is high enough and the surface temperature of cooling tubes remains approximately constant at 10°C.
- d) It is assumed that there is a convection heat transfer on the outer surface of the mold with a heat transfer coefficient of 2 W/m²K. The ambient air temperature is assumed to be 22 °C. The convection coefficient over a plate depends on the ambient fluid, velocity of fluid, length of the plate and temperature difference between the plate and ambient temperature. For the present case, length of the plate is 8.25 inch and temperature difference is about 28 °C. The velocity of the fluid is assumed to be 10 cm/s. On the basis of air properties and these variables, the convection coefficient is calculated below to be approximately 2 W/m²K:

Mean temperature of air = 309 K

Air properties at 309 K are as follows.

Density = 0.616 kg/m³

Kinematic viscosity = 47.85 m²/s

Thermal conductivity, k = 0.454 W/mK

Prandtl number, Pr = 0.68.

The Reynolds number of the flow is calculated to be 270.34.

So Nusselt number (Nu) can be calculated from Pohlhausen equation

(Chereources, 2008) as follows:

$$Nu = 0.664(Re)^{\frac{1}{2}}(Pr)^{\frac{1}{3}} = 9.60$$

$$\text{Then } h = \frac{Nu * k}{L} = 2.07 \text{ W/m}^2\text{K.}$$

- e) There will be pressurized air inside the mold so it is assumed that there is a convection heat transfer on the inside surface of the polymer layer with a heat transfer coefficient of $2 \text{ W/m}^2\text{K}$.

After the first cycle, the initial temperature of the mold for the second cycle is kept the same as the final temperature distribution of the mold at the end of the first cycle. The initial temperature of the mold at the start of third cycle is kept as its final temperature distribution at the end of second cycle and so on. The initial temperature of the parison is 204°C for every cycle. This process is repeated till the cycle repeats itself. The temperature profile of the polymer layer and the maximum temperature at the end of the cycle during the steady cyclic state is the desired output of the whole analysis. The maximum temperature within the final blown product should be less than the melting point of the polymer (HDPE, 135°C). The cycle is considered complete when the maximum temperature of the polymer part is no more than 110°C .

Table 2

Boundary conditions for the ALGOR simulations

Boundary condition	Value
Initial temperature of the mold (first cycle)	50 °C
Initial temperature of the parison	204 °C
Temperature of the surfaces of cooling channels	10 °C
Temperature inside the cavity	22 °C
Coefficient of heat convection on the out surface	2 W/m ² .K (2*10 ⁻⁶ W/mm ² .K)
Ambient temperature	22 °C
Coefficient of heat convection on the inner surface	2 W/m ² .K (2*10 ⁻⁶ W/mm ² .K)

4.3: Design of Cooling System using ALGOR

Solid Edge models with different designs of cooling tubes were tested for transient heat transfer for the above mentioned boundary conditions. The initial models had only cooling tubes but cooling tubes alone could not have the desired cooling affect because the distance between the cooling tubes and the center elevated portion of the mold surface is more than quarter inch. So a copper rod (0.25 inch diameter) or a heat pipe is used as a cooling pin. It was determined that a copper cooling pin would work just as well as a heat pipe in this application. The cooling pin is placed vertically at the centre of the mold (Figure 12). The top of the cooling pin is at a distance of quarter inch from the mold inner surface. The lower part of pin reaches the centre of the middle cooling

tube and is left open to coolant flow. Some of the designs which were tested are as follows:

- 1) 2 circular cooling tubes, 1 heat pipe and 5 straight tubes: Circular tubes are of quarter inch outer diameter and the outer diameter of straight tubes is 3/8 inch. The closest surface of the tubes is at a distance of quarter inch from the mold surface. The temperature profile at the end of the cycle is shown in Figure 12.

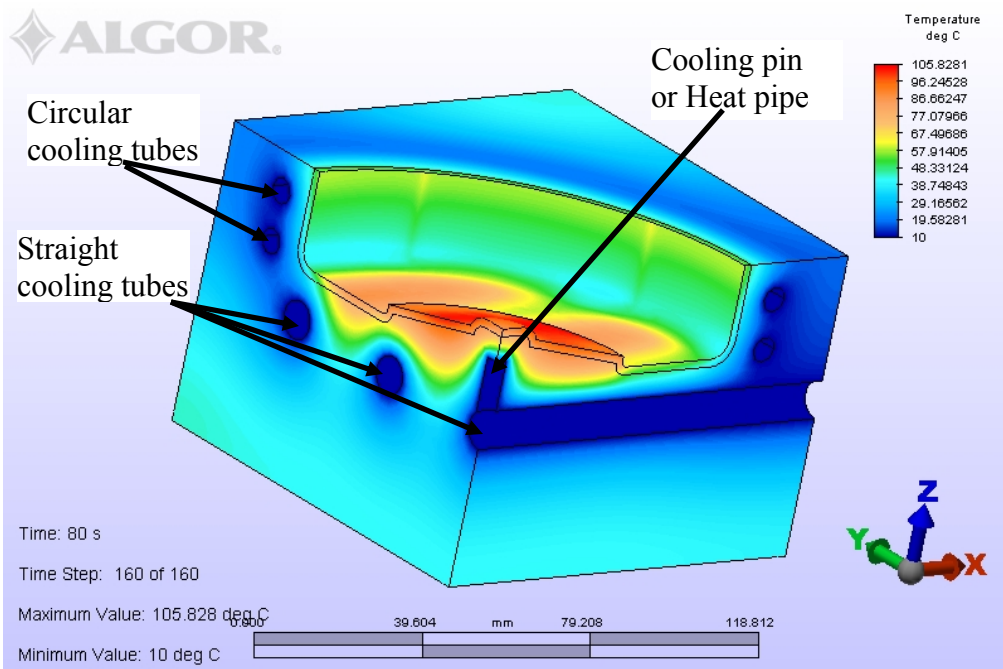


Figure 12: Temperature profile for design 1

- 2) 2 circular cooling tubes, 1 heat pipe and 7 straight tubes: Circular tubes are of quarter inch outer diameter and the outer diameter of straight tubes is 3/8 inch. The closest surface of the tubes is at a distance of quarter inch from the mold surface. The temperature profile at the end of the cycle is shown in Figure 13.

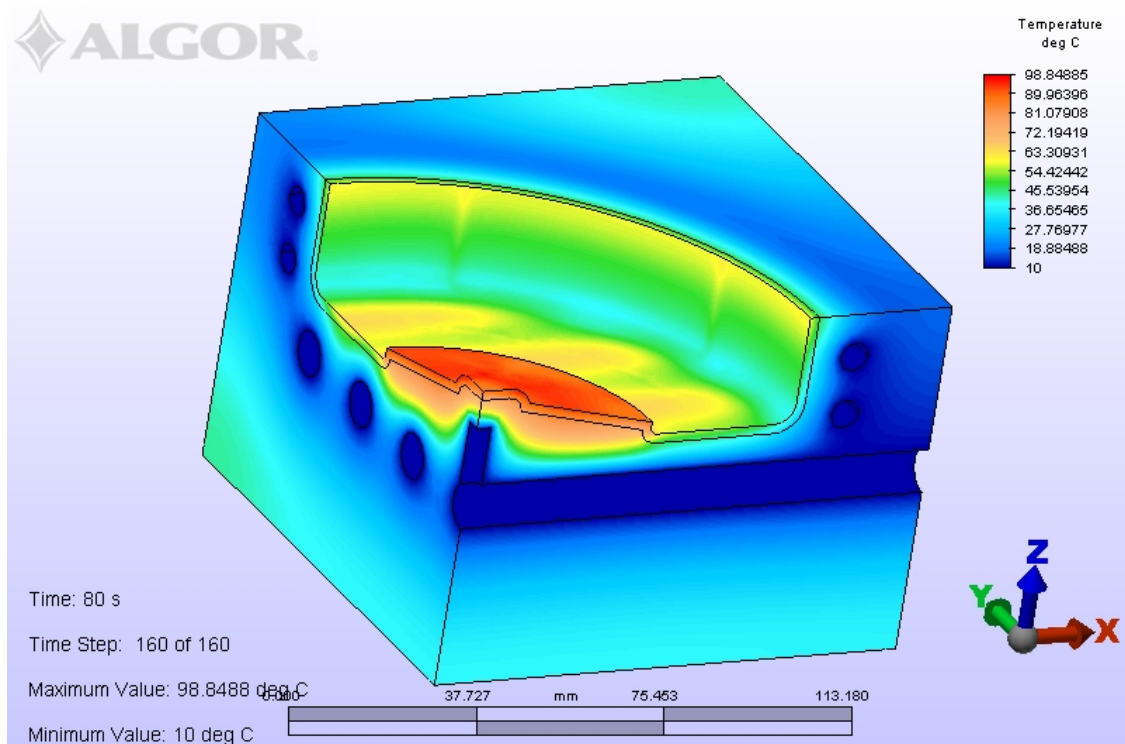


Figure 13: Temperature profile for design 2

- 3) 3 circular cooling tubes, 1 heat pipe and 5 straight tubes: Circular tubes are of quarter inch outer diameter and the outer diameter of straight tubes is 3/8 inch. The closest surface of the tubes is at a distance of quarter inch from the mold surface. The temperature profile at the end of the cycle is shown in Figure 14.

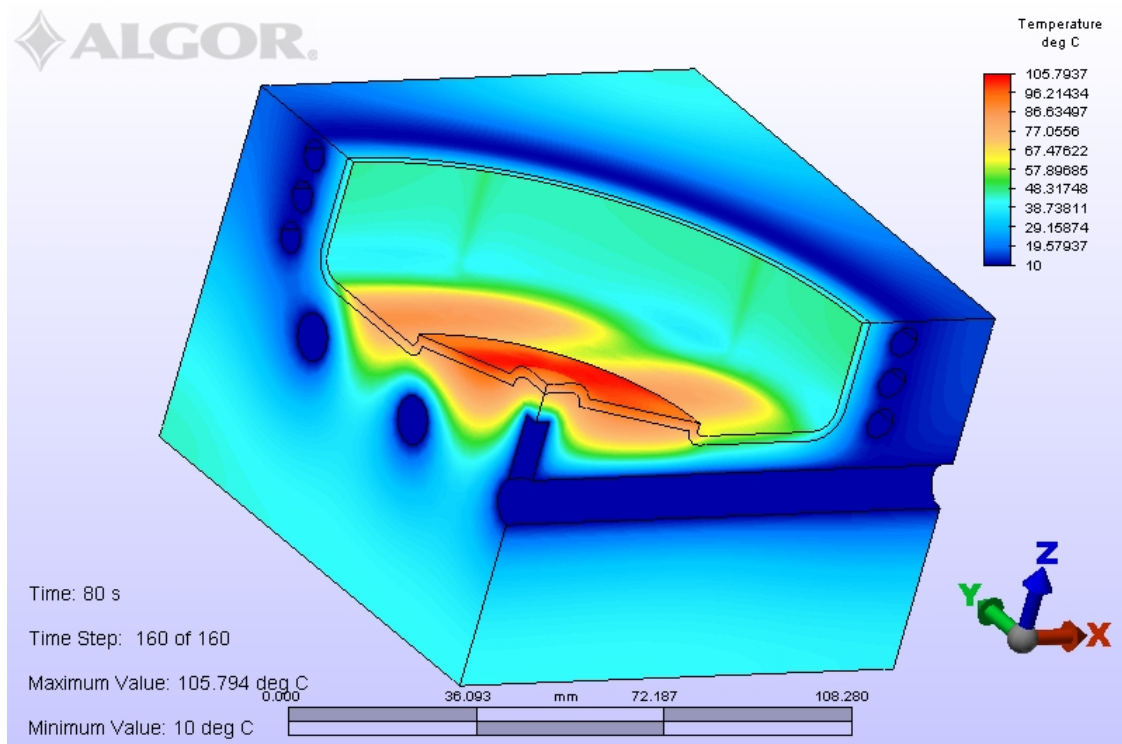


Figure 14: Temperature profile for design 3

- 4) 3 circular cooling tubes, 1 heat pipe and 7 straight tubes: Circular cooling tubes are of quarter inch outer diameter. The straight tubes are of 3/8 inch diameter except the middle tube, whose diameter is 0.5 inch. The closest surface of the tubes is at a distance of quarter inch from the mold surface. The temperature profile at the end of the cycle is shown in Figure 15.

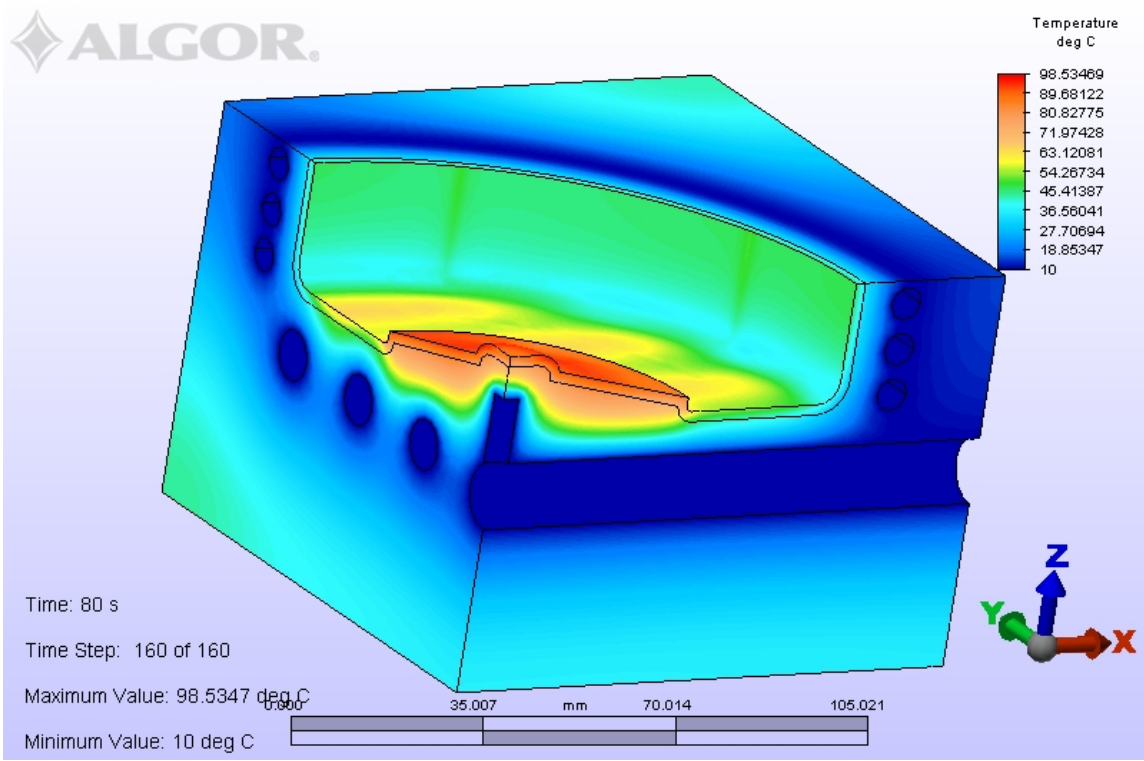


Figure 15: Temperature profile for design 4

5) 3 circular cooling tubes, 1 heat pipe and 5 straight tubes: Circular cooling tubes are of quarter inch outer diameter. The straight tubes are of half inch diameter. The closest surface of the tubes is at a distance of quarter inch from the mold surface. The temperature profile at the end of the cycle is shown in Figure 16.

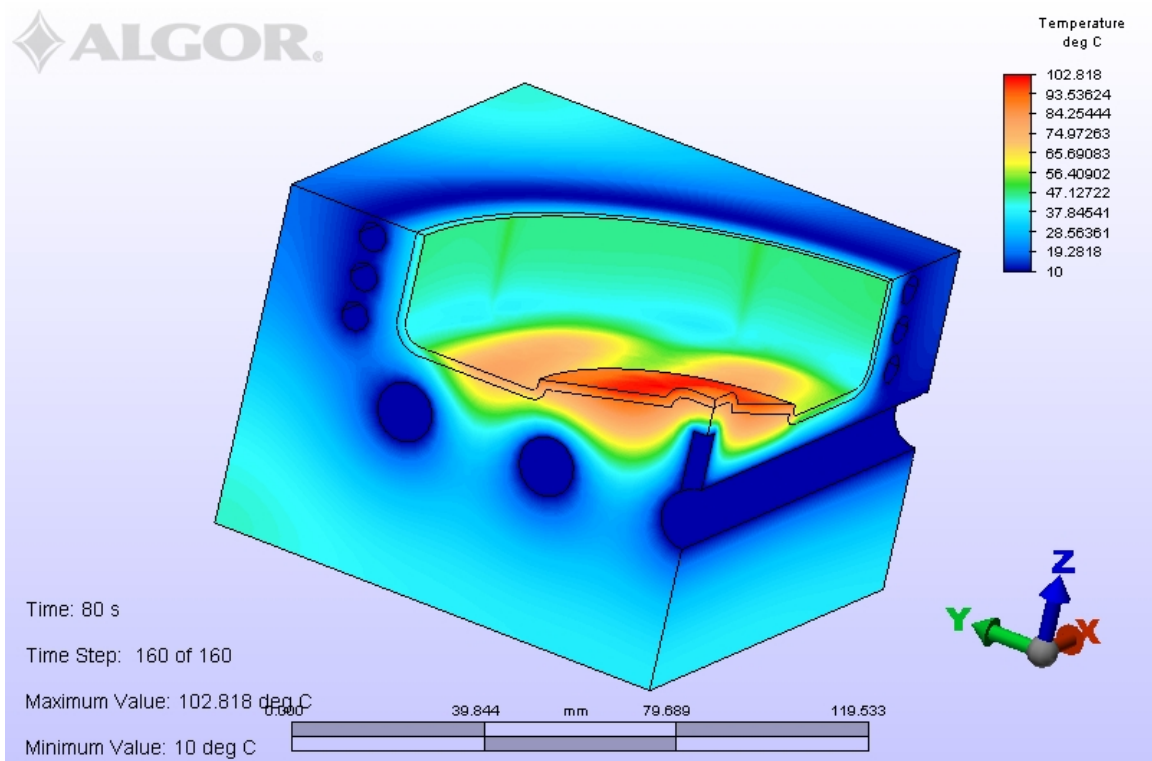


Figure 16: Temperature profile for design 5

- 6) 2 circular cooling tubes, 1 heat pipe and 5 straight tubes: Circular cooling tube is of quarter inch outer diameter. The straight tubes are of half inch diameter. The closest surface of the tubes is at a distance of quarter inch from the mold surface. The temperature profile at the end of the cycle is shown in Figure 17.

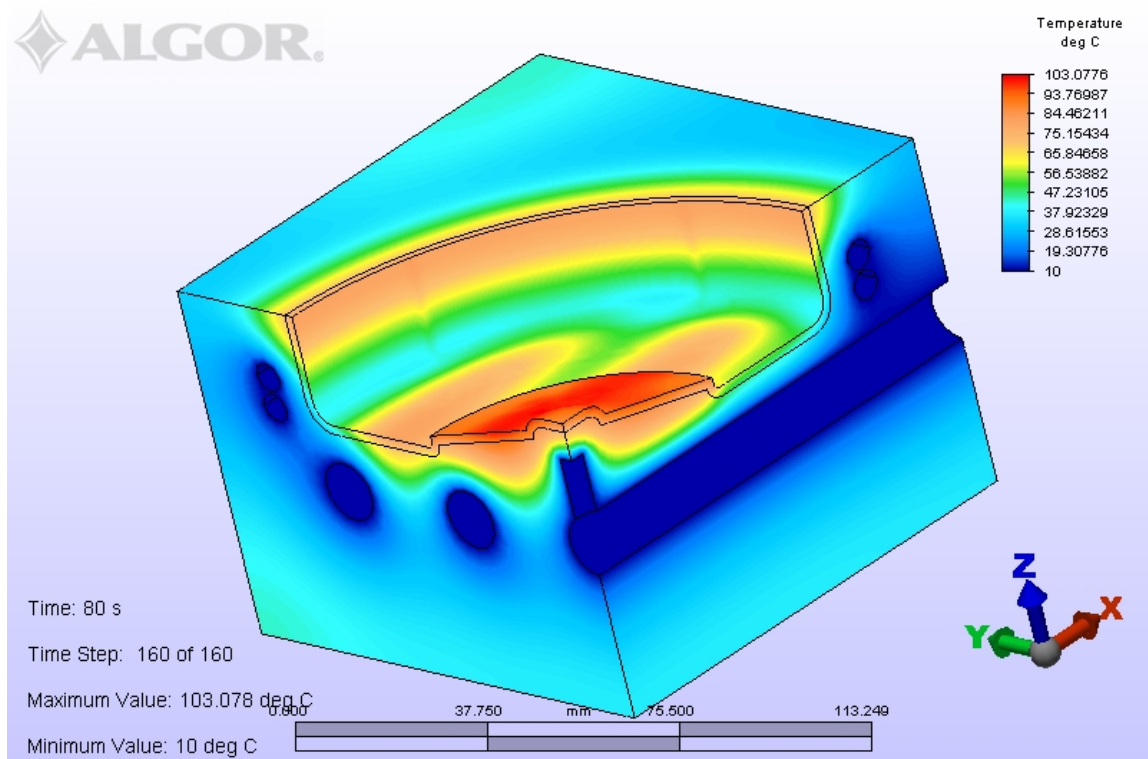


Figure 17: Temperature profile for design 6

- 7) 1 circular cooling tube, 1 heat pipe and 5 straight tubes: Circular cooling tube is of quarter inch outer diameter. The straight tubes are of half inch diameter. The closest surface of the tubes is at a distance of quarter inch from the mold surface. The temperature profile at the end of the cycle is shown in Figure 18.

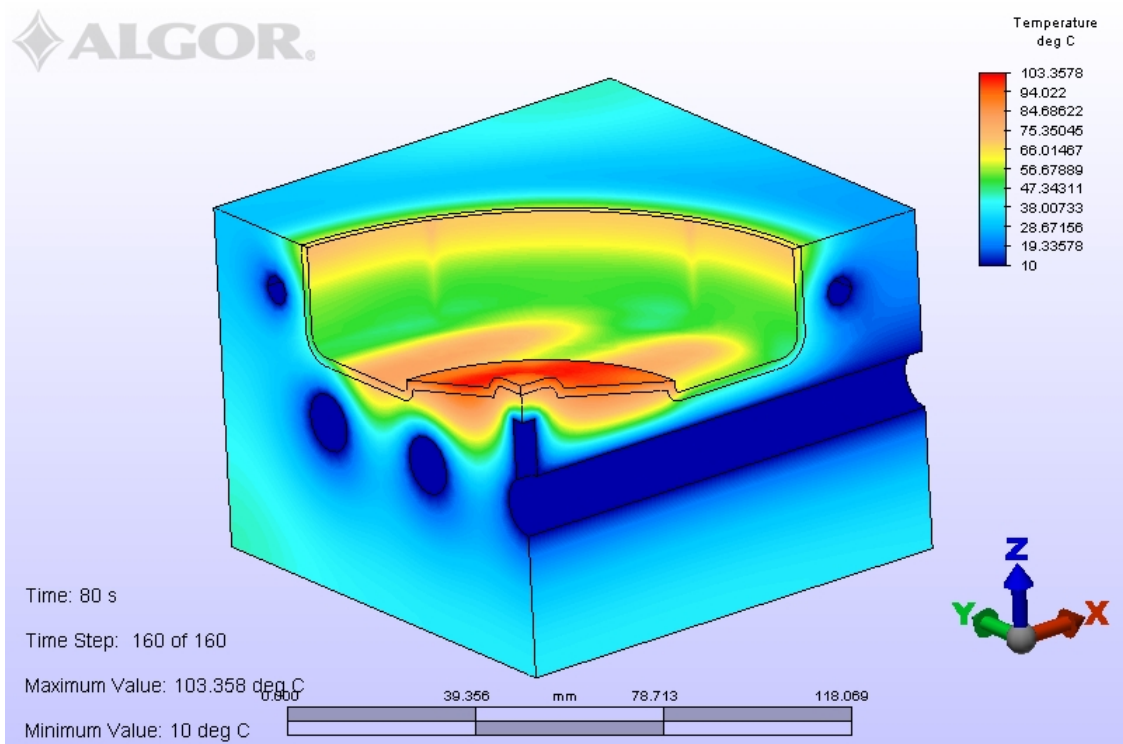


Figure 18: Temperature profile for design 7

In all the simulations, the temperature is found to be maximum at the centre elevated part of the mold. Therefore, this is the critical region that determines the cooling cycle time. It was decided that this elevated part of the mold would be removed from one side of the mold so that the heat transfer can be studied on ALGOR for a flat mold. The copper pin is not used for this mold. Two different designs of cooling channels are analyzed for a steady cyclic temperature profiles which are shown in Figure 19-20.

- 8) 2 circular cooling tube and 5 straight tubes: Circular cooling tubes are of quarter inch outer diameter. The straight tubes are of half inch diameter. The closest surface of the tubes is at a distance of quarter inch from the mold surface. The temperature profile at the end of the cycle is shown in Figure 19.

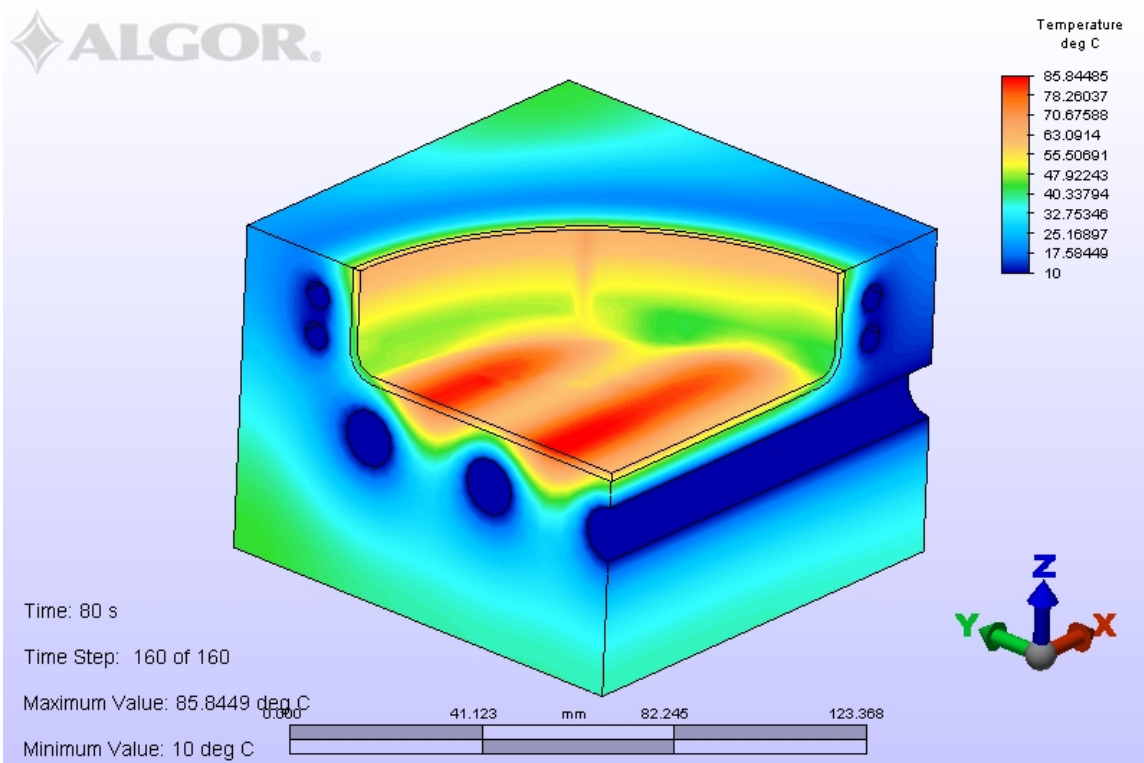


Figure 19: Temperature profile for design 8

- 9) 1 circular cooling tube and 5 straight tubes: Circular cooling tube is of quarter inch outer diameter. The straight tubes are of half inch diameter. The closest surface of the tubes is at a distance of quarter inch from the mold surface. The temperature profile at the end of the cycle is shown in Figure 20.

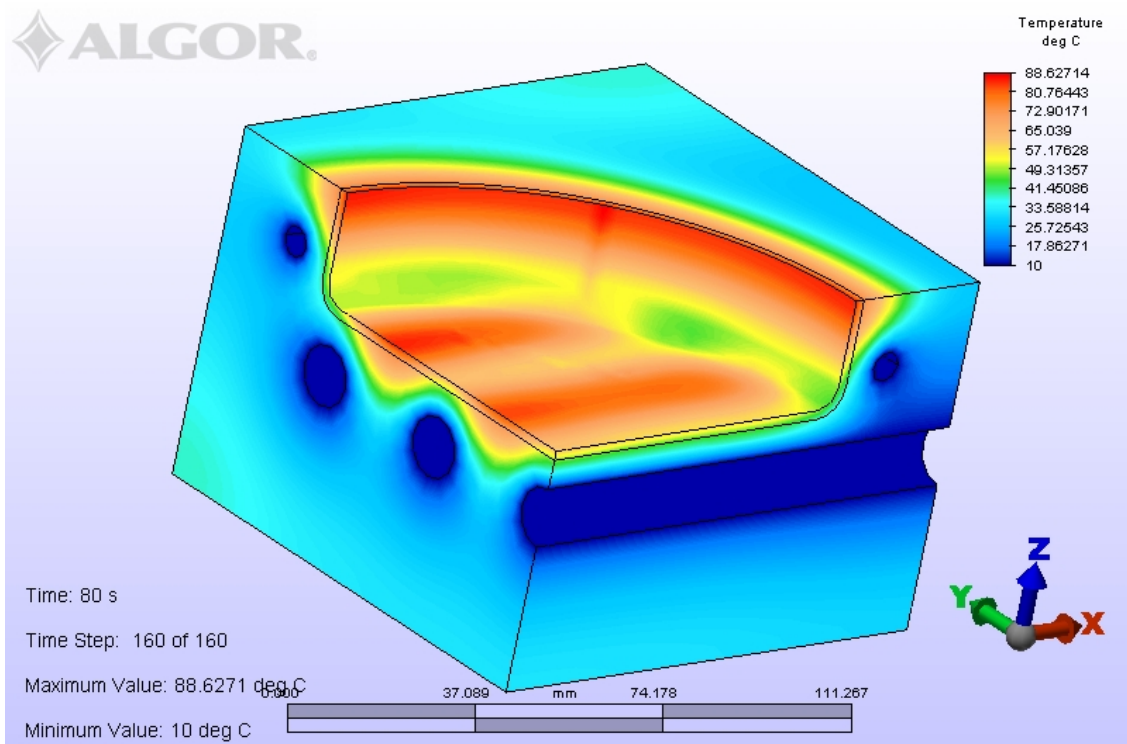


Figure 20: Temperature profile for design 9

The different designs considered are summarized in Table 3.

Table 3

Different designs of cooling channels

Design no.	Circular cooling tubes (0.25" diameter)	Straight cooling tubes	Heat Pin (0.25" diameter)	Maximum temperature (°C)
1	2	5 (3/8" diameter each)	1	105.828
2	2	7 (3/8" diameter each)	1	98.84
3	3	5 (3/8" diameter each)	1	105.794
4	3	7 (6 tubes of 3/8" diameter and middle of 0.5" diameter)	1	98.53
5	3	5 (0.5" diameter each)	1	102.818
6	2	5 (0.5" diameter each)	1	103.078
7	1	5 (0.5" diameter each)	1	103.358
8	2	5 (0.5" diameter each)	-	85.84
9	1	5 (0.5" diameter each)	-	88.62

4.4: Summary of Thermal Simulations

In all the simulations, the maximum temperature is found at the elevated part of the mold which determines the cycle time. The designs with two or three circular loops of cooling tubes at the top provide better cooling results (Figures 12 - 17) but if two loops of cooling coils are used then there will not be enough space left at the top of the mold to accommodate pinch off and extruder. The pinch off will be made by machining the top of the mold halves. If temperature profile and the ease of manufacturing are both taken into consideration, Design 7 (Figure 18) with 1 circular cooling tube and 5 straight tubes

produced favorable results. It can be seen that the maximum temperature in the system is about 103°C. This is below the maximum allowable temperature of 110°C so that the part can be ejected without affecting its geometric integrity.

For ALGOR simulations, the mold initial temperature is assumed to be 50 °C. The analysis is also repeated for a mold initial temperature of 22 °C and 35 °C. But the change in the maximum mold temperature at the end of a cycle during steady cyclic state was found to be negligible. This confirmed that the steady cyclic state is independent of the assumed value of mold initial temperature.

The convection coefficient on the inner surface is assumed to be a constant value of 2 W/m².K for ease of calculation. This convection coefficient can be much higher on the inner surface because parison is made to expand by using pressurized air. Figure 21 shows the variation of maximum temperature at the end of the cycle with increase in convection coefficient on the inner surface.

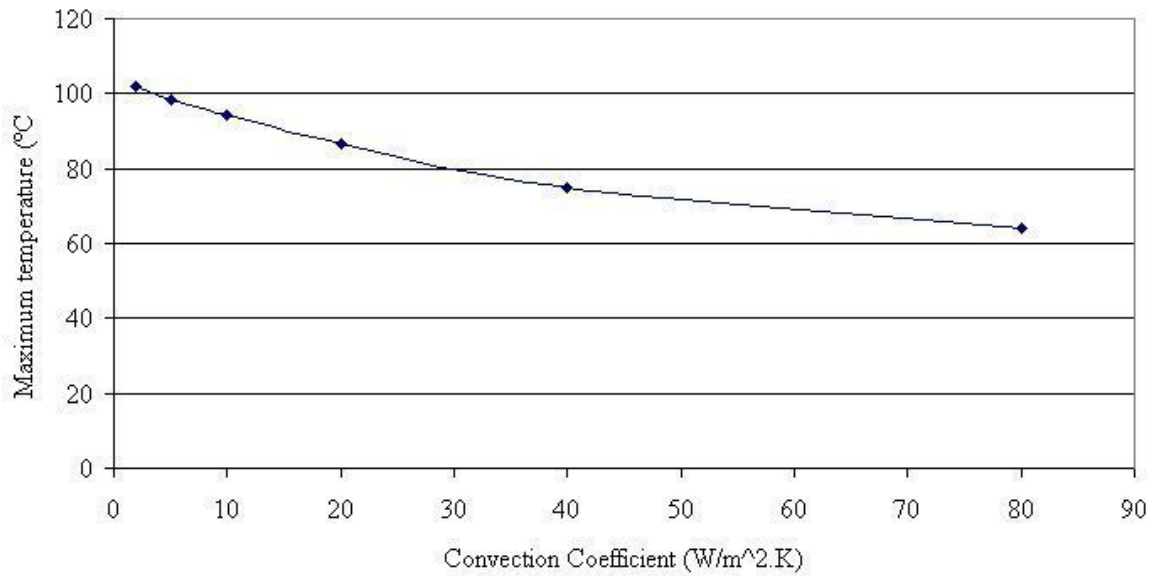


Figure 21: Variation of maximum temperature at the end of the cycle during steady cyclic state with increase in convection coefficient on the inner surface

A parametric study was also carried out to determine the effect of increasing cycle time on the cooling of the mold. With increasing cycle time, the cooling requirements are less stringent since the product temperature has sufficient time to cool down. Figure 22 shows the maximum temperature at the end of the cycle for different cycle times. Based on these results, a cycle time of 80 seconds was selected.

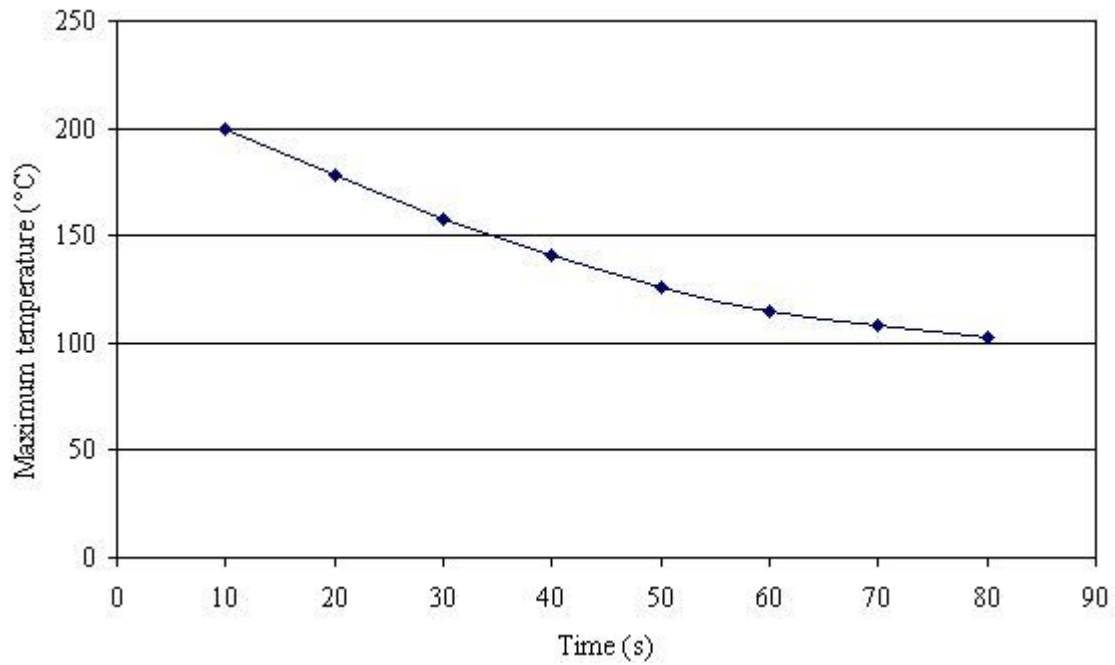


Figure 22: Maximum temperature vs time during a cycle for design no. 7

The maximum temperature at the end of the cycle for a flat mold comes out to be 88° C. The flat mold design does not have a cooling pin. Therefore, the flat mold does not require a cooling pin to cool the mold below the ejection temperature.

CHAPTER 5: MANUFACTURING OF NANOCOMPOSITE BLOW MOLD

After the mold design is selected by ALGOR simulations, the mold core manufactured in chapter 3 was machined accordingly. However, there were additional conditions for the mold that must be taken into consideration. An attachment would be connected to the mold so that the parison tube can be inserted into the mold cavity by an extruder. A pinch off must be made in the mold core by machining (Figure 23). So there has to be some gap at the top of the both mold halves to accommodate extruder and pinch off. The design with two or three loops of cooling tubes makes it difficult to accommodate pinch off and extruder so the design with one loop of cooling tube was selected. This design has a space of 0.5 inch at the top to accommodate additional machining. The design with 1 loop of cooling tube of quarter inch diameter and 5 straight tubes of half inch diameter was selected from designs analyzed in chapter 4 (Figure 18).

Nanocomposite mold core was manufactured as described in the chapter 3. The cooling channels are to be machined in the nanocomposite core according to the chosen design (Design 7) which can be summarized as follows:

1. Circular cooling channels: A circular groove with a width of quarter inch and a depth of half inch is made around the mold cavity. The distance between the cooling channel surface and mold surface is kept as quarter inch. Copper cooling tube with a diameter of quarter inch is placed in the machined groove. After fitting the copper tubing, the groove is filled with the nanocomposite material that was used in making the mold.

2. Straight cooling channels: 5 straight channels, each with a diameter of half inch, are made below the mold cavity. The distance between the cooling channel surface and mold surface is kept as quarter inch. The straight channels are fitted with metal inserts at both ends to connect them to cooling water source.
3. Cooling pin: A hole is drilled at the centre of the core from its back. A cooling pin with a diameter of quarter inch is pushed into this blind hole with a snug fit.

The engineering drawing of the preliminary design of the mold cooling system is shown below (Figure 23 and Figure 24).

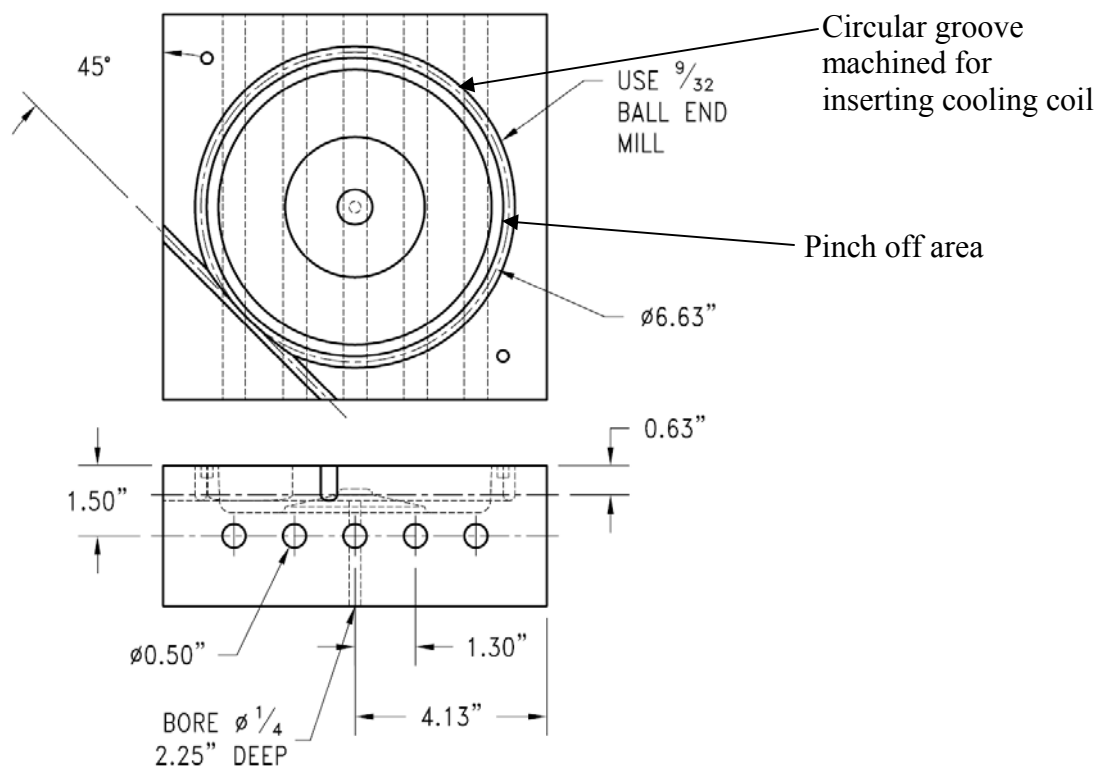


Figure 23: Orthographic views of the blow mold for final machining (Source: Center for Advanced Materials Processing (CAMP), Ohio University)

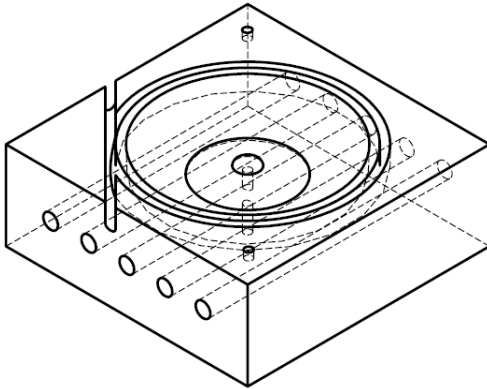


Figure 24: Isometric view of the blow mold core for final machining (Source: Center for Advanced Materials Processing (CAMP), Ohio University)

One straight groove was made at each end so that the nanocomposite mold core can be gripped properly in the mold (Figure 25).



Figure 25: Nanocomposite mold core with cooling channels and grooves at two sides for gripping the mold structure (Source: Center for Advanced Materials Processing (CAMP), Ohio University)

After machining the cooling channels, the nanocomposite mold core was cast into a low cost fiber reinforced composite block (Figure 26) which was necessary to make the tooling large enough to fit into smallest blow molding machine available at the testing facility.

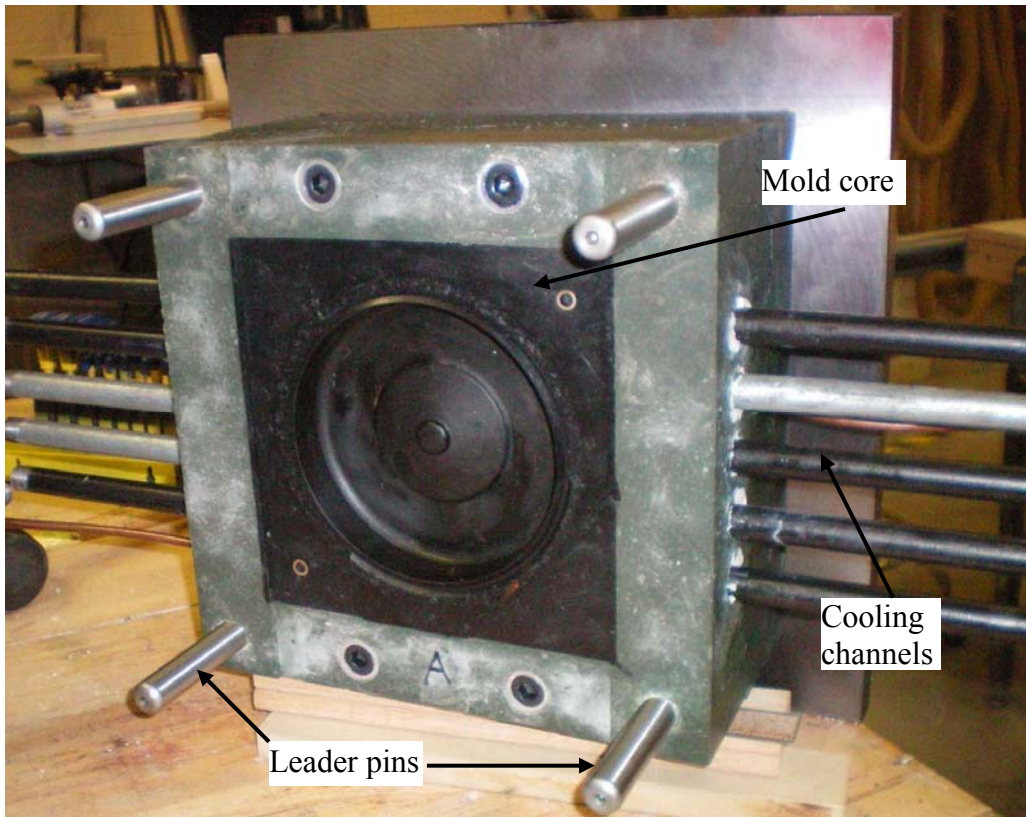


Figure 26: Mold half with nanocomposite mold core (Source: Center for Advanced Materials Processing (CAMP), Ohio University)

Another half of the mold is made with a flat surface (Figure 27) to study the effect of the geometry on the cooling of the part. The cooling channels for this half with flat surface are made in the same way except that there is no cooling pin used in this half.

Only the cooling channel around and the beneath the mold cavity are used for the cooling of the blow molded product.

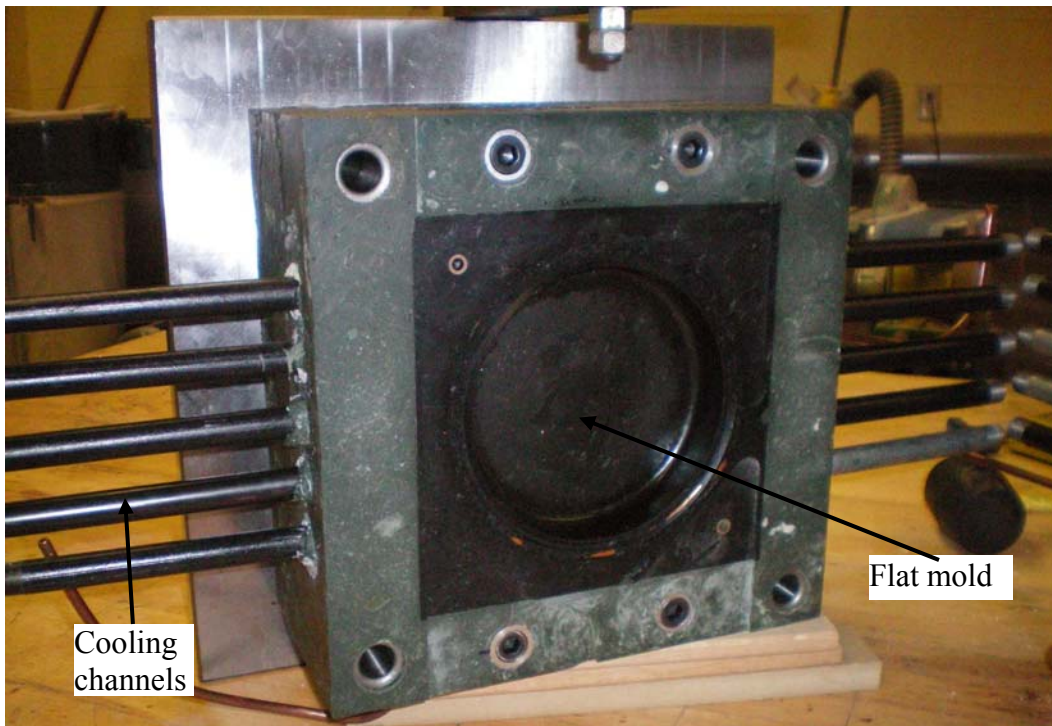


Figure 27: Mold half with flat surface (Source: Center for Advanced Materials Processing (CAMP), Ohio University)

The final cast blocks were also fitted with leader pins and mounting plates (Figure 28).

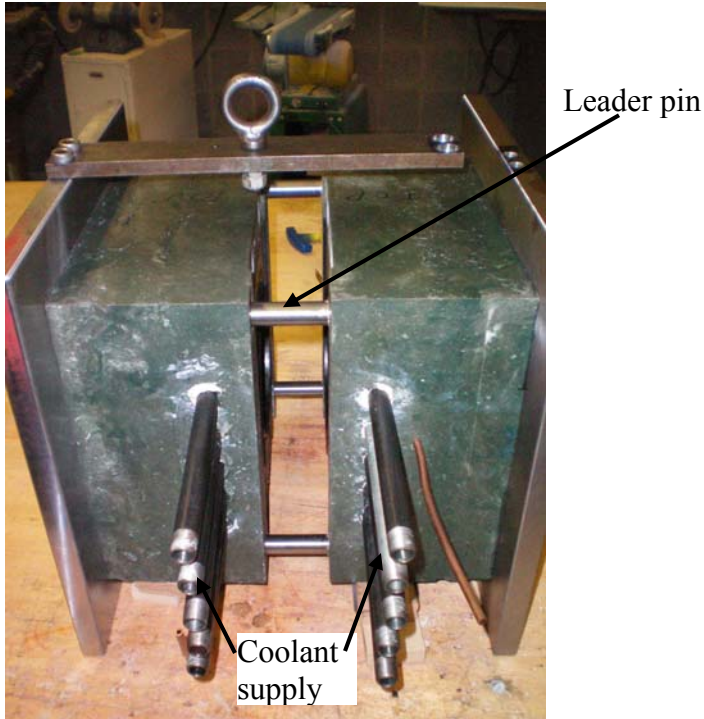


Figure 28: Mold halves positioned by leader pins (Source: Center for Advanced Materials Processing (CAMP), Ohio University)

It should also be noted that the cooling channels could also be designed as part of the mold core while making the core. This would save time and money spent on the machining process. This will be taken into account if this design is put into commercial use. The final step is to insert the blow mold air injection needle which will be done later at the blow molding facility.

CHAPTER 6: STRESS ANALYSIS IN POLYFLOW

6.1: Solid Edge Model

The design with the best cooling performance within the manufacturing constraints has already been selected on the basis of ALGOR simulations. Then POLYFLOW simulations are performed for the analysis of mechanical properties and deformations of the final product. A Solid Edge model is created along with the parison which is shown in Figure 29.

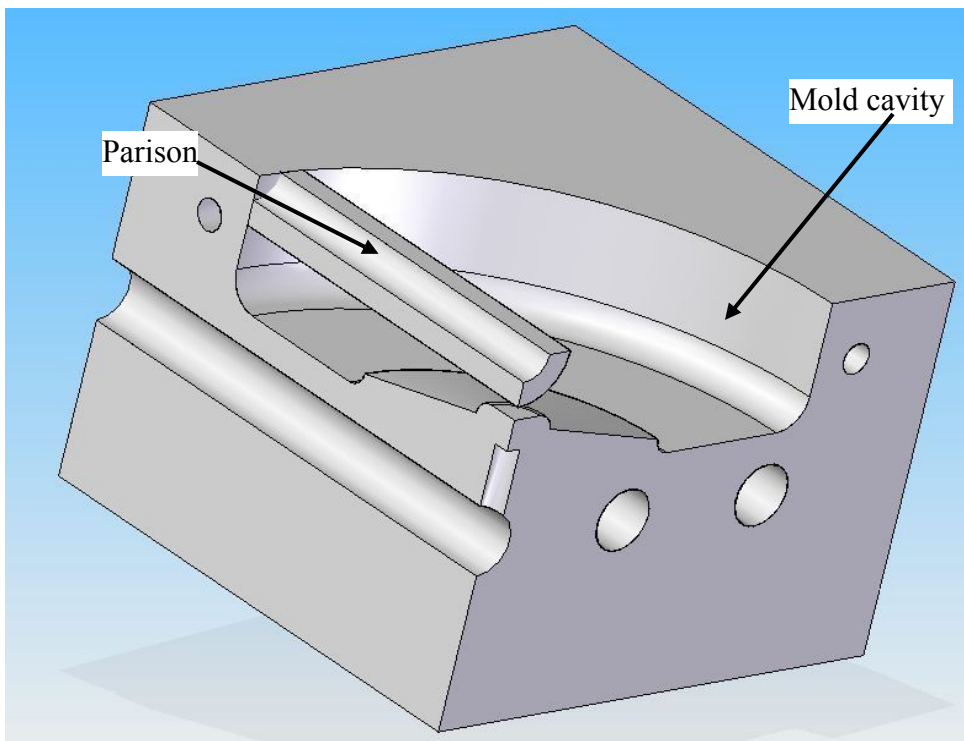


Figure 29: Solid Edge model for mold along with the parison

This Solid Edge file is then exported as *.iges file and then imported into Gambit, which is used for meshing of the model. The meshed model is then exported as a *.neu

file and imported into POLYFLOW which is then used for the analysis of the blow molding simulations.

6.2: Gambit Meshing

The Solid Edge geometry is imported into Gambit. There may be some errors in the geometry due to some limitations in Solid Edge. There might also be a difference in default tolerance settings of Solid Edge and Gambit. So the imported geometry is healed before meshing by merging of faces, edges and volumes. The model is meshed into tetrahedral elements. Parison is meshed using a size of 0.1 and the mold is meshed using a size of 0.25 (see Figure. 30). The parison is meshed into 1763 tetrahedral elements with 564 nodes and the mold is meshed into 18620 tetrahedral elements with 4121 nodes. Boundary types are also defined in Gambit. Boundary types have to given an index so that they can be identified in POLYFLOW by the given index. In addition to boundary types, continuum types (fluid or solid) are also defined for the solid edge model. There are only two continuum types for the current model, namely mold and the parison. Then the mesh file is exported as a neutral file.

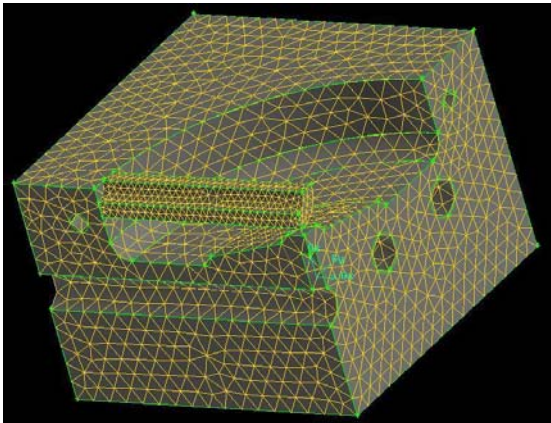


Figure 30: Meshed model in Gambit

6.3 Parison Thickness

Initial thickness of the parison is unknown at this point. Many trials were made with parisons of different thicknesses. A post-processor for tracking of material points is created just to be sure that the initial thickness of the parison has the sufficient material and there are no holes/tears in the final blow molded wheel.

6.3.1: Tracking of Material Movement

The model was first analyzed to check that the flow of the material is occurring as expected. A cycle time of 35 seconds is used to blow the parison. No temperature calculations are performed for the mold or for the parison at this stage. The mold is assigned a uniform constant temperature. The viscosity of the parison material (HDPE) is considered to be a constant, $\eta = 3 \times 10^6$ Pa.s. The results for tracking of material points at different instants during the cycle time can be seen in Figure 31. This figure confirms that material is continuous and there are no tears in the final blow molded wheel.

Once the required thickness of the parison for the blow molded product without any tears/holes has been decided, the next step is to study the mechanical properties of the final product. A stress postprocessor for the POLYFLOW model is created to calculate the variation of principle stresses in the model while blowing the parison.

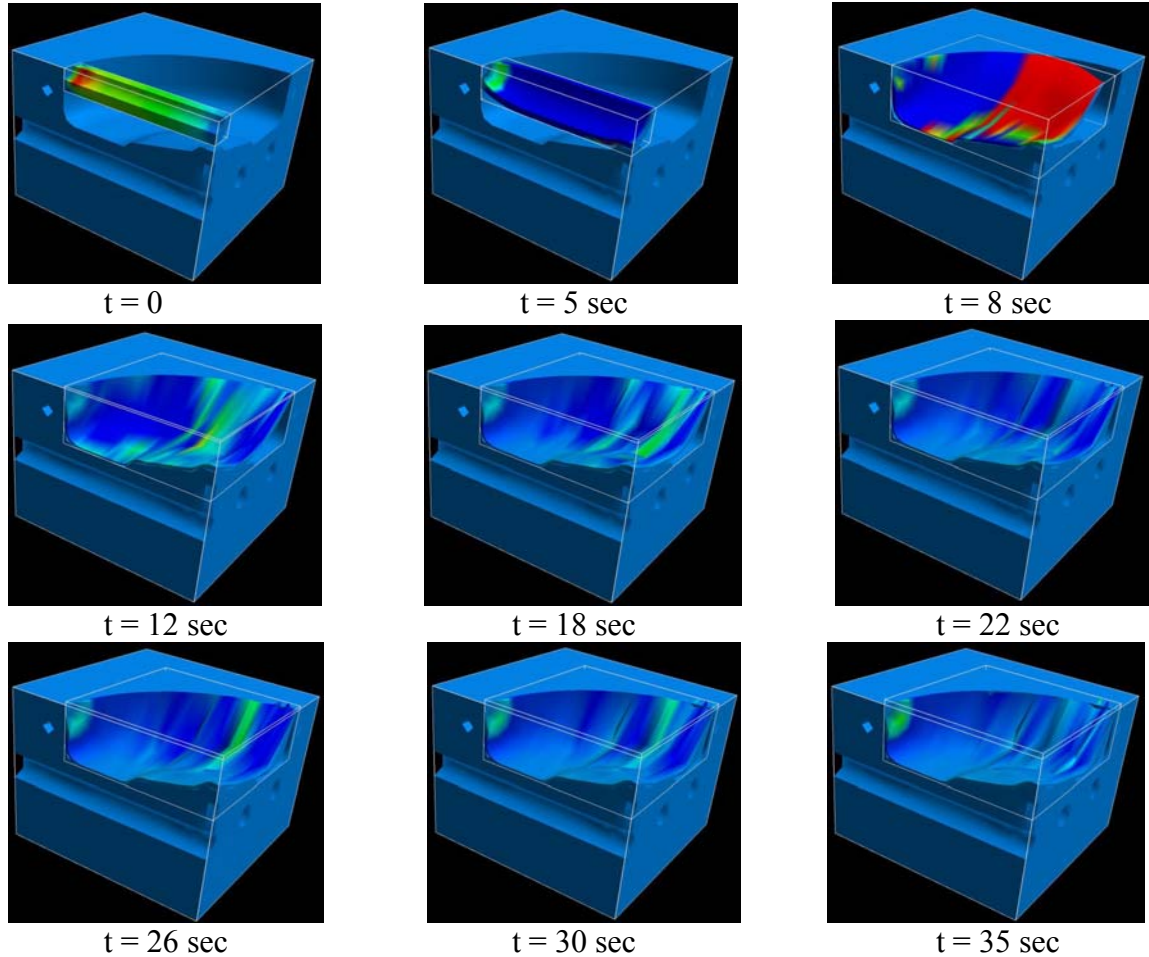


Figure 31: Tracking of material movement at different times during a blow cycle

Since the POLYFLOW simulation is starting after the pinch off, the maximum thickness of the parison is limited by the size of the mold. As the height of the elevated portion at the centre is 0.5 inch, it puts a constraint on the maximum thickness of the parison to be 0.5 inch for a solid parison with internal diameter of zero. The parison dimensions used for the subsequent simulations are decided on the basis of iterations and can be seen in Figure 32.

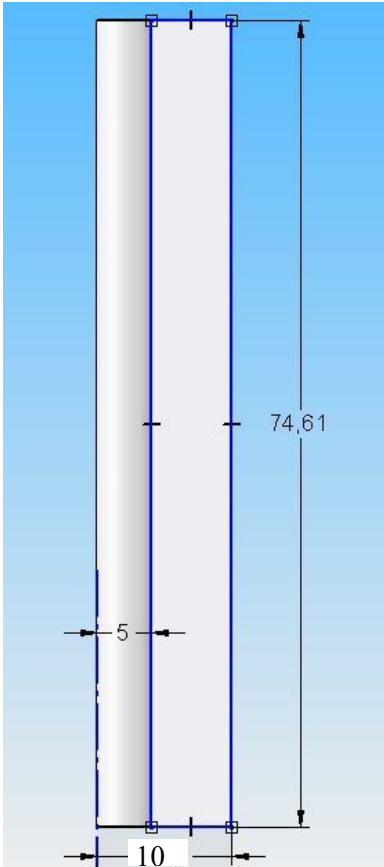


Figure 32: Parison dimensions (All the dimensions are in mm)

6.4: Material Properties for POLYFLOW Model

Material properties which are common to each of POLYFLOW models are summarized in the table 4.

Table 4

Material properties common to all POLYFLOW models

Property	Nanocomposite Mold	HDPE
Thermal Conductivity, k	1.653 W/mK	0.3966 W/mK
Heat Capacity, c_p	1090 J/Kg/K	2300 J/Kg/K
Density, ρ	1440 Kg/m ³	1382.9 Kg/m ³
Coefficient of Thermal Expansion, α	0.00006 inch/inch/°C	
Viscosity, η		3000000 Pa.s

Viscous heating is being neglected in all the models. Gravity forces and inertia are taken into account. Viscosity is considered to be temperature independent for the simplicity of the model.

6.5: Boundary Conditions

6.5.1: Flow Boundary Conditions

The flow boundary conditions applied for the models are as follows

1. The inner surface of the parison is considered to be a free surface (Figure 33). A constant pressure of 650000 Pa is applied on the inner surface. Ideally the pressure applied will decrease with the increase in volume due to blowing of the parison. Pressure is assumed to be constant for the simplification of the model. A reasonable pressure value that would be successful is obtained by trial and error to be 650000 Pa (95 psi), which is normally used for this operation at a commercial blow molding facility.

2. As only one-eighth of the model is being considered due to symmetry, there are displacement constraints on the radial cutting surfaces of the parison, Figure 33. These two radial surfaces can decrease their thicknesses but they will always be in the same plane. The same constraint is applicable to the surface which cuts the parison in two halves. These three faces are selected to be planes of symmetry.

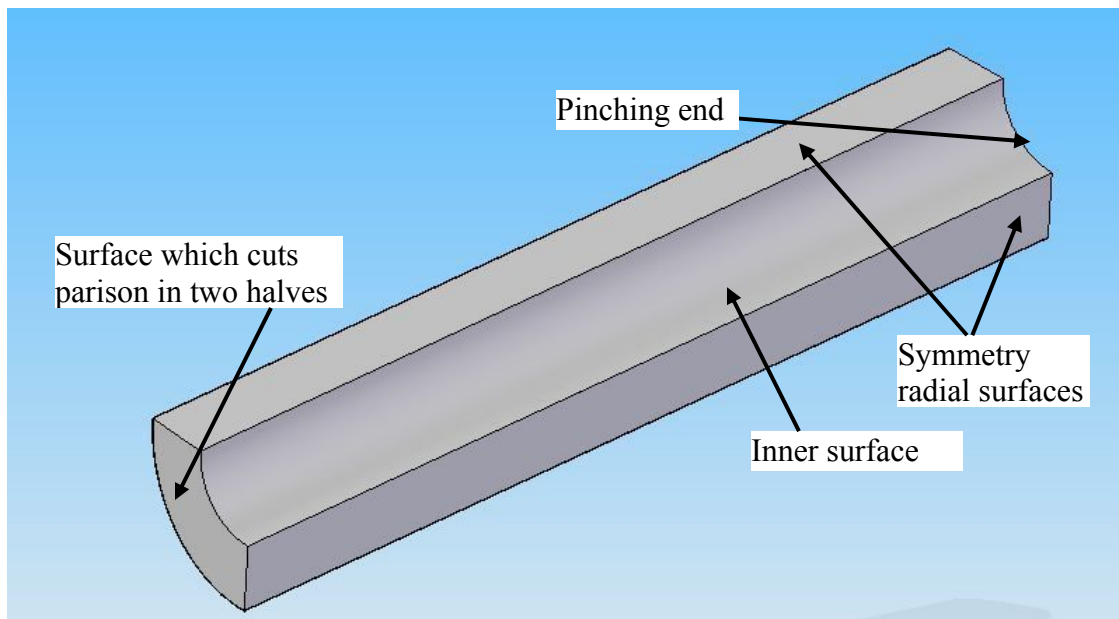


Figure 33: Parison boundaries

3. Outer surface of the parison is also considered to be a free surface (see Figure. 34).
4. As the parison blows, its outer surface will come into contact with the mold.

A contact problem is defined with the parameters in Table 5.

Table 5

Contact problem parameters

Parameter	Value
Alpha	1×10^9
Slipping Coefficient	1×10^9
Penalty Coefficient	1×10^9
Penetration Accuracy	3×10^{-2}
Element Dilation	3×10^{-2}

The given value of slipping coefficient assures that the velocity of the polymer is zero after contact. The penalty coefficient assures that the radial velocity of the expanding parison is equal to the velocity of mold in the same direction, which is zero. Otherwise, lower values of penalty coefficient will result in a theoretical penetration of polymer into mold walls. Penetration accuracy limits the maximum penetration allowed for the final product. Higher values will result in a rough surface of the final product. Elements of the mold are dilated for contact detection. The maximum dilation is given by the last parameter in Table 5.

6.5.2: Thermal Boundary Conditions

If an isothermal analysis is being considered, then it is not required to define any temperature boundary conditions. It is required to define only a uniform constant temperature of the mold which is defined to be 103 °C from the previous ALGOR analysis (maximum temperature at the end of each cycle).

If a non isothermal analysis is being considered then the temperature boundary conditions are as follows:

1. The inner surface of parison is at 25 °C.
2. The outer surface of the parison is at 153 °C.
3. The pinching end of the parison is at 103 °C.
4. Three flat faces of the parison and corresponding in-plane faces of the mold are defined as insulated boundaries or symmetry faces.
5. The surface of the cooling tubes is at 10 °C.
6. The outer surface of the mold is assumed to be equal to the room temperature. It is considered to be 25 °C.
7. The contact surface of the mold is at 103 °C.

6.6: Remeshing

The parison will undergo a large amount of deformation while blowing. The elements will elongate in length and will become very thin. The internal angles will increase/decrease and elements may not remain valid FEA elements. The degree of skew (shear) is also a matter of concern. So the meshing which was done initially will not be good for further analysis and remeshing is necessary for accurate results. POLYFLOW recommends Lagrangian, Shell or Thompson transformation for 3D blow molding analysis. As the current model is made up of tetrahedral elements only, Lagrangian meshing and Thompson transformation option have been selected for remeshing. The remeshing is defined with the parameters defined in Table 6.

Table 6

Parameters for Lagrangian and Thompson remeshing techniques

Serial no.	Condition	Value
1	Minimum interior angle	5°
2	Maximum interior angle	175°
3	Maximum bend	10
4	Maximum aspect ratio	50
5	Maximum skew	10

The remeshing process via Thompson transformation begins with a definition of global coordinate system. The number of coordinates in the global coordinate system should be equal to the number of coordinates in the original model. The global coordinate definition for the current model can be seen in Figure 34. G1, G2 and G3 are three global coordinates defined for remeshing of parison during the process. When the mesh deforms while blowing of parison, POLYFLOW will relocate the nodes such that their global coordinates remain the same. All the six faces are remeshed using tangential remeshing.

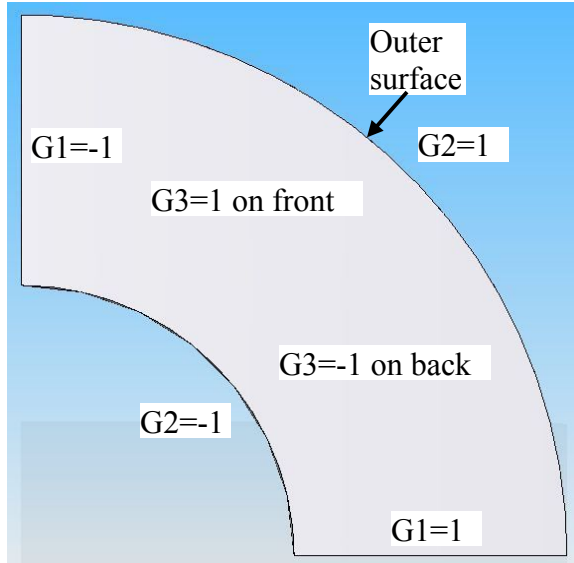


Figure 34: Global coordinates for parison remeshing

6.7: POLYFLOW Models

POLYFLOW offers a large number of models, however only a few are available for the current analysis. The current problem is modeled as a time dependent FEM task. Different kinds of models are tried for the analysis under study. These are listed as follows:

- 1) Generalized Newtonian isothermal flow problem with constant viscosity.
- 2) Generalized Newtonian isothermal flow problem with viscosity as a function of shear rate (Cross law).
- 3) Generalized Newtonian non-isothermal flow problem with viscosity as a function of shear rate (Cross law).
- 4) Integral viscoelastic isothermal KBKZ shell model (2-D membrane model).
- 5) Integral viscoelastic non-isothermal KBKZ shell model (3-D model).

This analysis is represented by a 3-D viscoelastic non-isothermal model but the function of viscosity as a function of shear rate is unknown at this point. So a model with constant viscosity has to be considered first. The choice of the function of viscosity depends on the values of shear rate. The shear rate values are calculated using a model with constant viscosity and the viscosity function is chosen according to the range of shear rate values. Then the shear rate values of the subsequent viscoelastic models are checked for the validity of function for viscosity.

The 3-D integral viscoelastic model with a stress postprocessor failed to converge. So it was decided to start from a very simple model with constant viscosity which has to be solved to get the viscosity function and then complexity of the problem is increased step by step. First, the simplest Newtonian model is used and the non linearity is added. The problem converged for a 2-D membrane model (KBKZ viscoelastic model). KBKZ model has already been used for the similar types of problems (Debbaut & Rekers, 1999).

According to POLYFLOW manual, the best model for the current analysis would be Giesekus model but it is not used due to the lack of material constants required for the definition of the model.

6.7.1: Function for Viscosity

The choice of viscosity function depends on the range of shear rate values. The shear rate variation is first calculated from the simplest model, i.e. Newtonian isothermal flow problem with constant viscosity and with no mold calculations. Then a function for viscosity is chosen accordingly. Then shear rate variation is checked for each model to see if the choice of the viscosity function is consistent.

POLYFLOW allows only a limited number of functions for shear dependence of viscosity. Modified Cross law is used for this analysis. From the analysis of constant viscosity model, it was found that shear rate varies from 0 to 1.5 (Figure. 35).

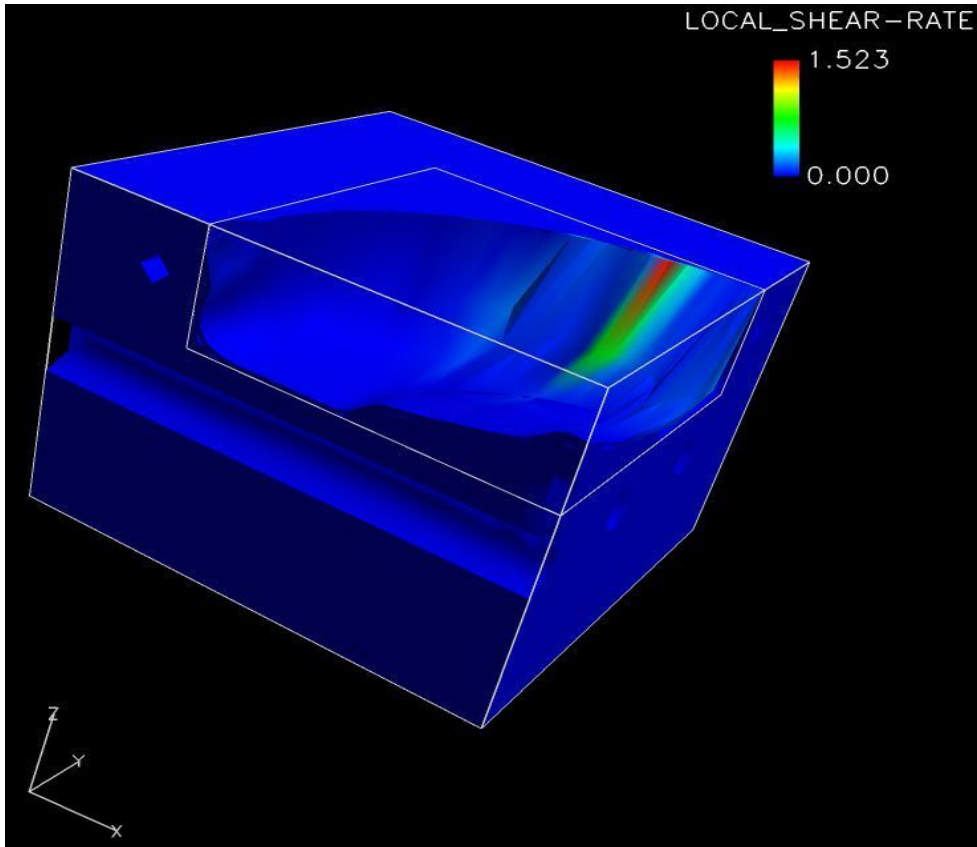


Figure 35: Variation of shear rate for constant viscosity model

The maximum shear rate occurs in the area farthest from the centre of the mold. This is the area of maximum deformation. The modified Cross law is known to provide good results for low values of shear rate; and the shear rate is in the low range. The modified Cross law for viscosity is given as:

$$\eta = \frac{\eta_0}{(1 + \lambda\dot{\gamma})^m} \quad (3)$$

where:

η_0 is the zero shear viscosity.

λ is the natural time.

$\dot{\gamma}$ is the shear rate.

M is the Cross law index.

Viscosity for different shear rates of HDPE is calculated using an empirical formula (Vinogradov & Malkinov, 1966). The empirical relation is

$$\frac{\eta_{\max}}{\eta} = 1 + A_1(D\eta_{\max})^\alpha + A_2(D\eta_{\max})^{2\alpha} \quad (4)$$

Where the following values are for HDPE:

η_{\max} is the zero shear rate viscosity

D is the shear rate

$$\alpha = 0.355$$

$$A_1 = 6.12 \times 10^{-2.645}$$

$$A_2 = 2.85 \times 10^{-3.645}$$

A number of viscosity points are calculated for different shear rates from equation (4) and then an equation for a best fit modified Cross law curve is derived from those data points. The parameters for Cross law equation derived are given in Table 7.

Table 7

Parameters for modified Cross law

Parameter name	Value of parameter
Zero shear rate viscosity, η_0	3×10^6 Pa.s
Natural time, λ	1
Cross law index, m	0.3

6.8: Stress Postprocessor

An inelastic stress post processor is available in POLYFLOW to calculate the variation of stress tensor and its eigenvalues (principle stress values) for the product during the process. This can be used to estimate the residual stresses present in the final product; such stresses can lead to warping and deformation. This analysis is done for different models, as discussed below.

6.8.1: Newtonian Models

For a generalized Newtonian flow, three equations are solved: momentum equation, incompressibility equation and the energy equation (POLYFLOW manual, version 3.12). The temperature, velocity and pressure fields are fully coupled. The energy equation is solved only for non isothermal flows.

The form of the momentum equations (POLYFLOW manual, version 3.12) is

$$-\nabla p + \nabla \cdot \vec{T} + \vec{f} = \rho \vec{a} \quad (5)$$

where:

p = pressure

\vec{T} = extra-stress tensor

\vec{f} = volume force

ρ = density

\vec{a} = acceleration

The incompressibility equation (POLYFLOW manual, version 3.12) is:

$$\nabla \cdot \vec{v} = 0 \quad (6)$$

where \vec{v} is velocity.

The energy equation (POLYFLOW manual, version 3.12) is:

$$\rho c_p \frac{D\vec{T}}{Dt} = r - \nabla \cdot \vec{q} + (\sigma \vec{D}) \quad (7)$$

where:

σ = the Cauchy stress tensor

\vec{D} = rate of deformation tensor

The following three models follow the Newtonian constitutive law:

(a) Isothermal Flow Problem with Constant Viscosity

The flow is considered to be Newtonian with constant viscosity. The flow is isothermal, i.e. there is no heat transfer while the parison is blowing. The mold temperature is assumed to be constant for this analysis. No thermal calculations are done for the mold.

For the above mentioned boundary conditions, the resultant principle stresses variation at the end of the cycle time for this isothermal model is shown in Figures 36-38.

POLYFLOW results give the fields for the three principle stresses ($\sigma_1, \sigma_2, \sigma_3$).

POLYFLOW does not provide the Von-Mises stress field and it has to be calculated manually. As the range of the principle stress values is too big, the exact value of the principle stress cannot be obtained directly. So the maximum Von-Mises stress is calculated for the maximum values of the principle stresses. It is unlikely that this stress is actually present at any point, but it provides an upper limit to the value of the Von-Mises stress.

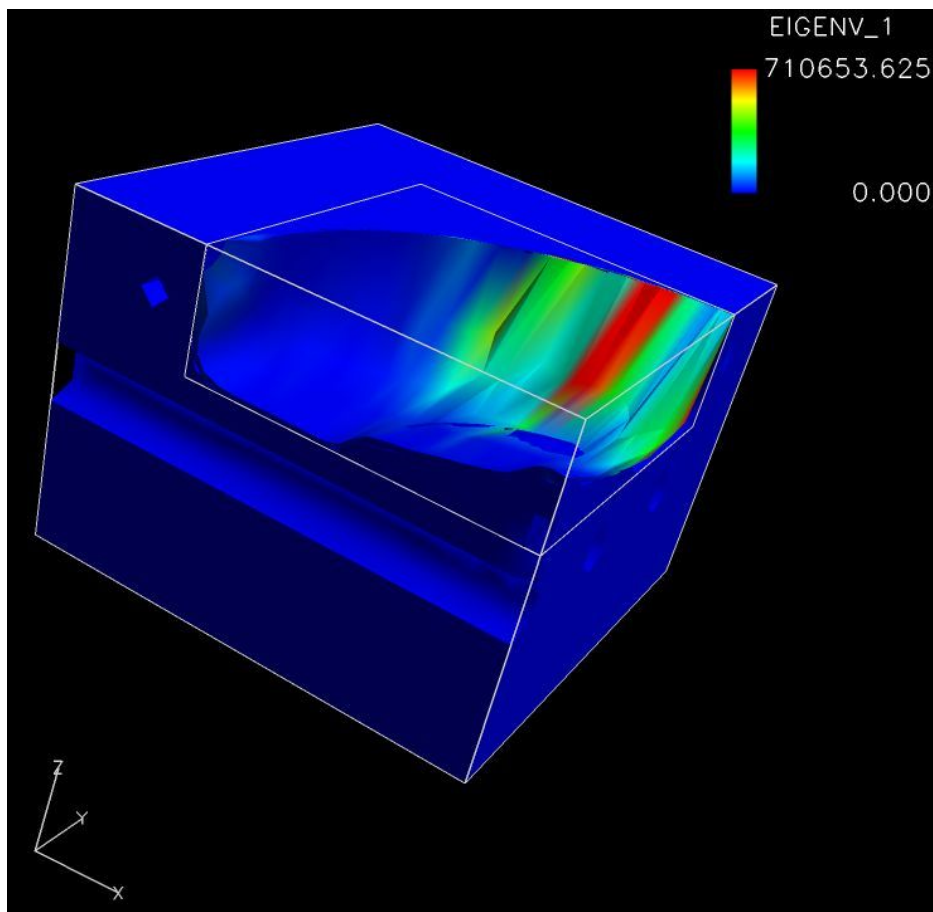


Figure 36: Variation of σ_1 for Newtonian model with constant viscosity

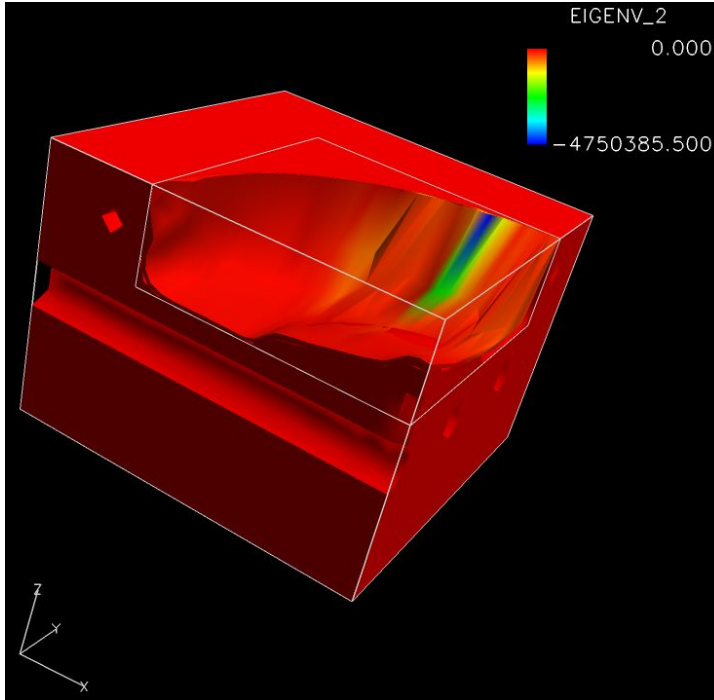


Figure 37: Variation of σ_2 for Newtonian model with constant viscosity

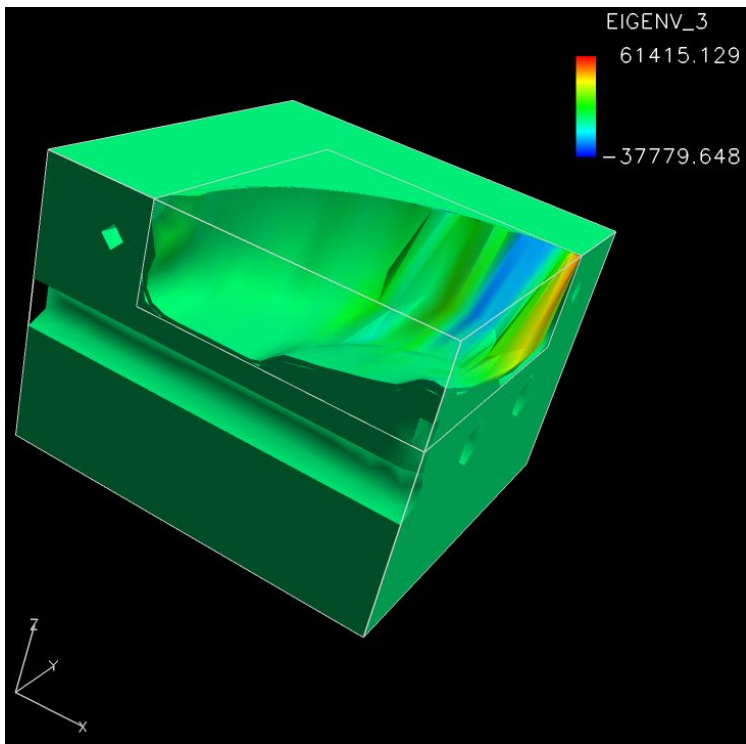


Figure 38: Variation of σ_3 for Newtonian model with constant viscosity

σ_1 varies from 0 to 710.86 kPa, σ_2 varies from -4.75 MPa to 0 Pa and σ_3 varies from -37.79 kPa to -61.15 kPa. The maximum principle stress values for this model are $\sigma_1 = 710 \text{ kPa}$, $\sigma_2 = -61 \text{ kPa}$, and $\sigma_3 = -4.75 \text{ MPa}$.

According to the model, the principle stress is higher in the areas farthest from the center. This non uniformity in stress values may lead to warping and a deformed final product. The maximum value of Von-Mises stress can be calculated to be

$$\begin{aligned}\sigma_{\text{von mises}} &= \frac{\sqrt{2}}{2} \sqrt{(\sigma_1 - \sigma_2)^2 + (\sigma_2 - \sigma_3)^2 + (\sigma_3 - \sigma_1)^2} \\ &= 5.11 \text{ MPa}\end{aligned}\quad (8)$$

The tensile strength of HDPE is equal to 26 MPa. So the part is not expected to fail due to the stresses produced by the process. The maximum shear stress according to Tresca's theory is equal to 5.46 MPa. The Young modulus of HDPE is approximately 1000 MPa. Therefore, Von Mises strain is equal to:

$$\text{Von Mises strain} = \frac{\text{Von Mises Stress}}{\text{Young Modulus}} = 0.0051 \quad (9)$$

The shear modulus is equal to 750 MPa which results in a maximum shear strain of:

$$\text{Shear strain} = \frac{\text{Shear Stress}}{\text{Shear Modulus}} = 0.00728 \quad (10)$$

(b) Generalized Newtonian Isothermal Flow Problem

The flow is considered to be Newtonian with viscosity as a function of shear rate (modified Cross law). The flow is isothermal, i.e. there is no heat transfer while the

parison is blowing. The mold temperature is assumed to be constant for this analysis. No thermal calculations are done for the mold. The variation of the shear strain rate is shown in Figure 39.

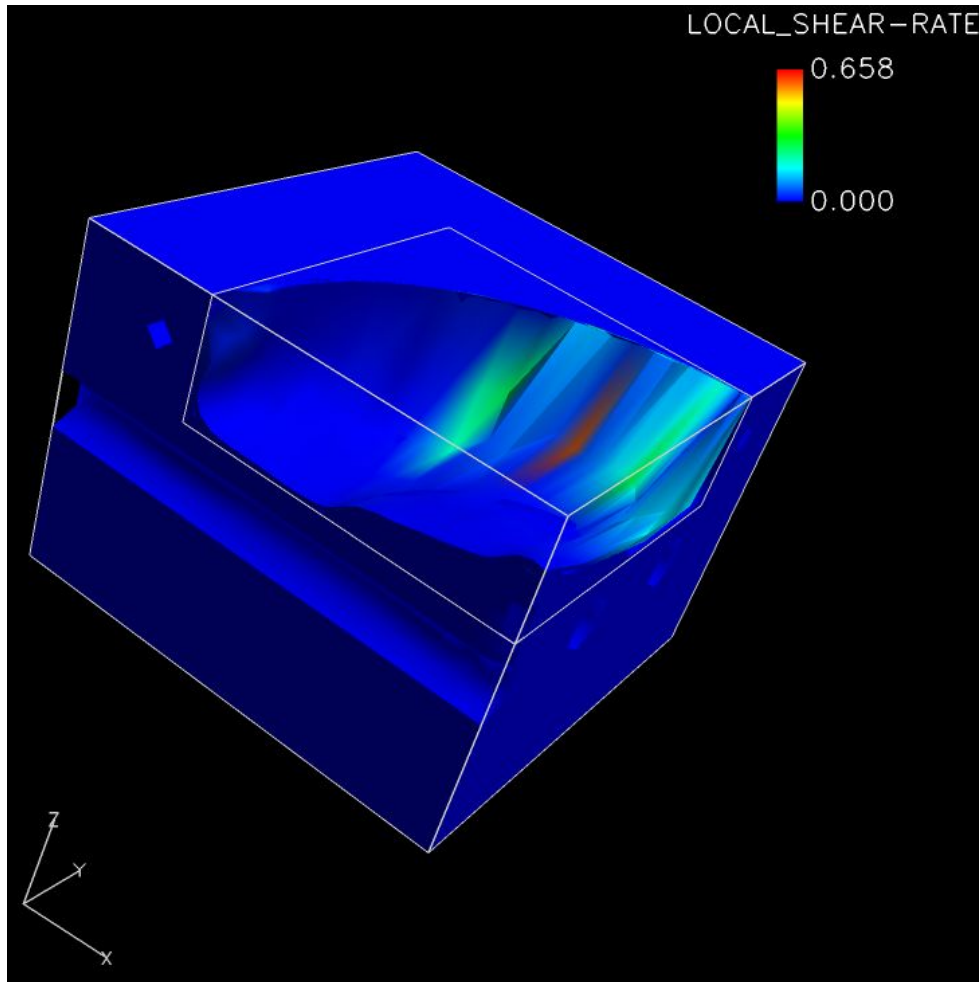


Figure 39: Variation of shear rate for Newtonian isothermal model with variable viscosity

The maximum value of shear strain rate is 0.658. So it seems to be quite reasonable to use modified Cross law for the viscosity as a function of shear strain rate. The variation of principle stresses for this model can be seen in the Figures 40-42.

From Figures 40-42, the maximum principle stresses come out to be $\sigma_1 = 759 \text{ kPa}$, $\sigma_2 = 57 \text{ kPa}$, and $\sigma_3 = -1.32 \text{ MPa}$. Using equation 8, Von-Mises stress comes out to be equal to 1.83 MPa.

Maximum shear stress is equal to 2.079 MPa. So the final product has a Von-Mises strain and shear strain values of 0.0018 and 0.0027 respectively.

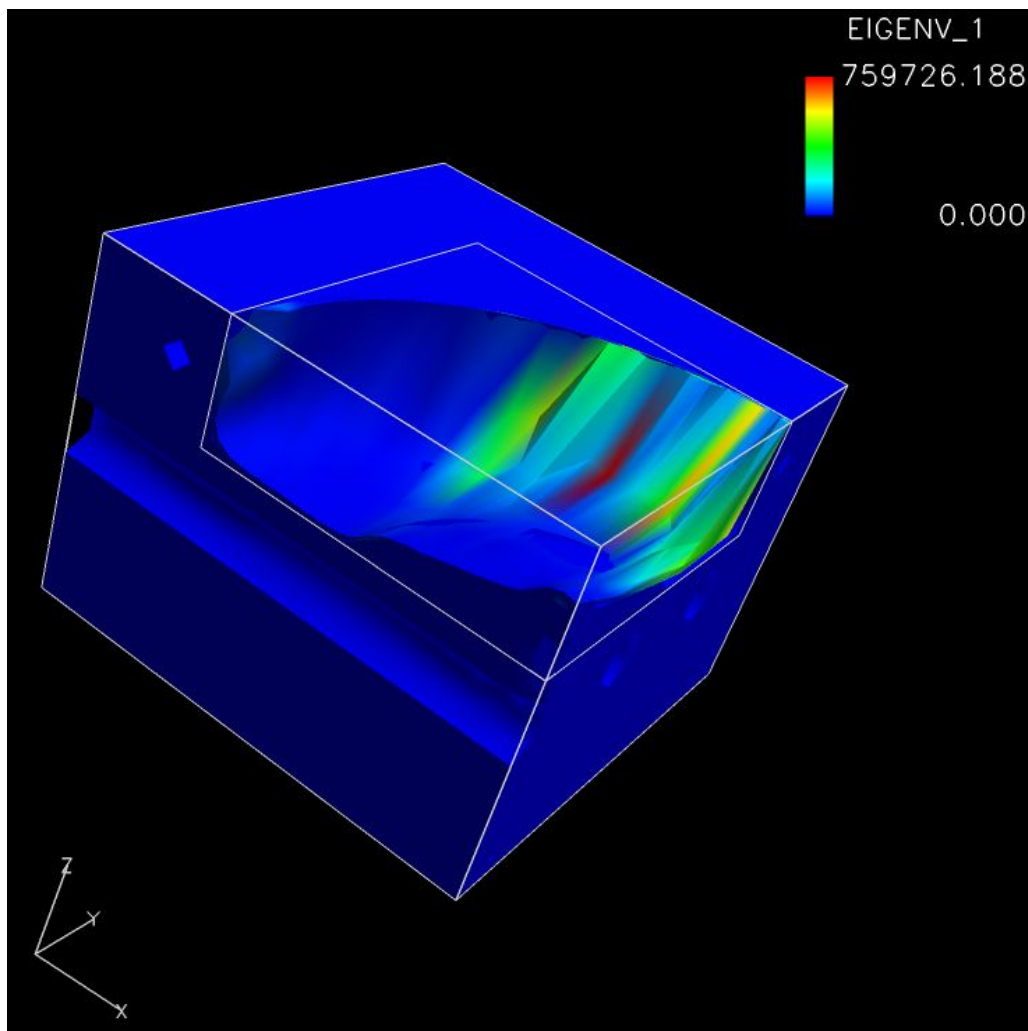


Figure 40: Variation of σ_1 for Newtonian isothermal model with variable viscosity

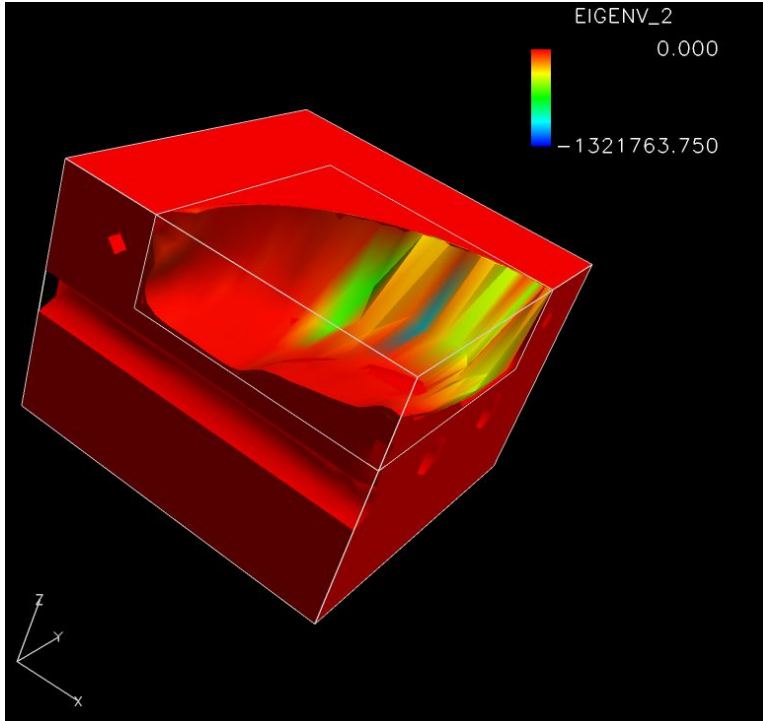


Figure 41: Variation of σ_2 for Newtonian isothermal model with variable viscosity

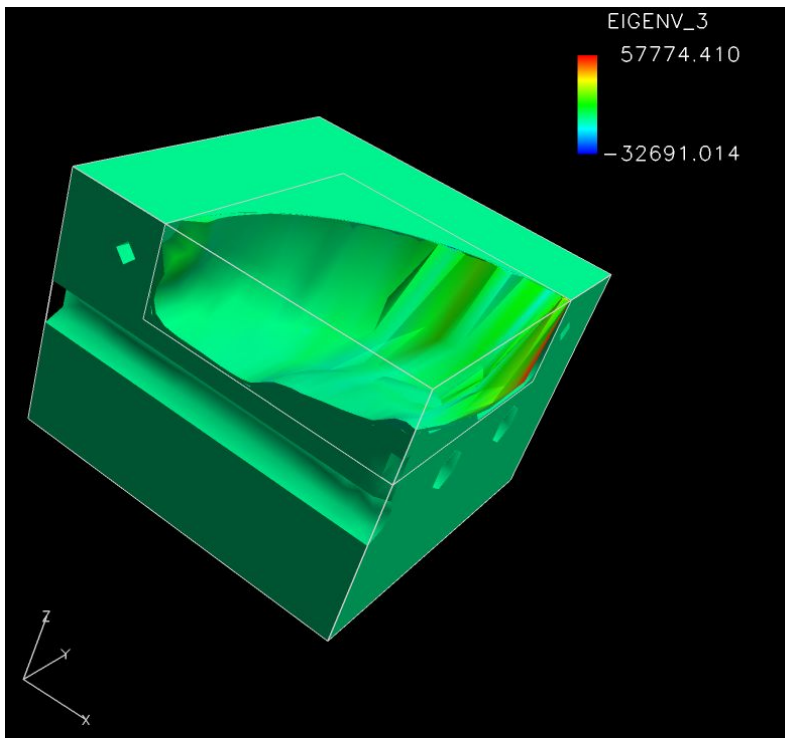


Figure 42: Variation of σ_3 for Newtonian isothermal model with variable viscosity

(c) Generalized Newtonian Non-isothermal Flow Problem

The flow is considered to be Newtonian with viscosity as a function of shear rate (modified Cross law). The flow is non-isothermal so mold thermal calculations are performed for the temperature field with the above mentioned boundary conditions. The variation of shear strain rate is shown in Figure 43.

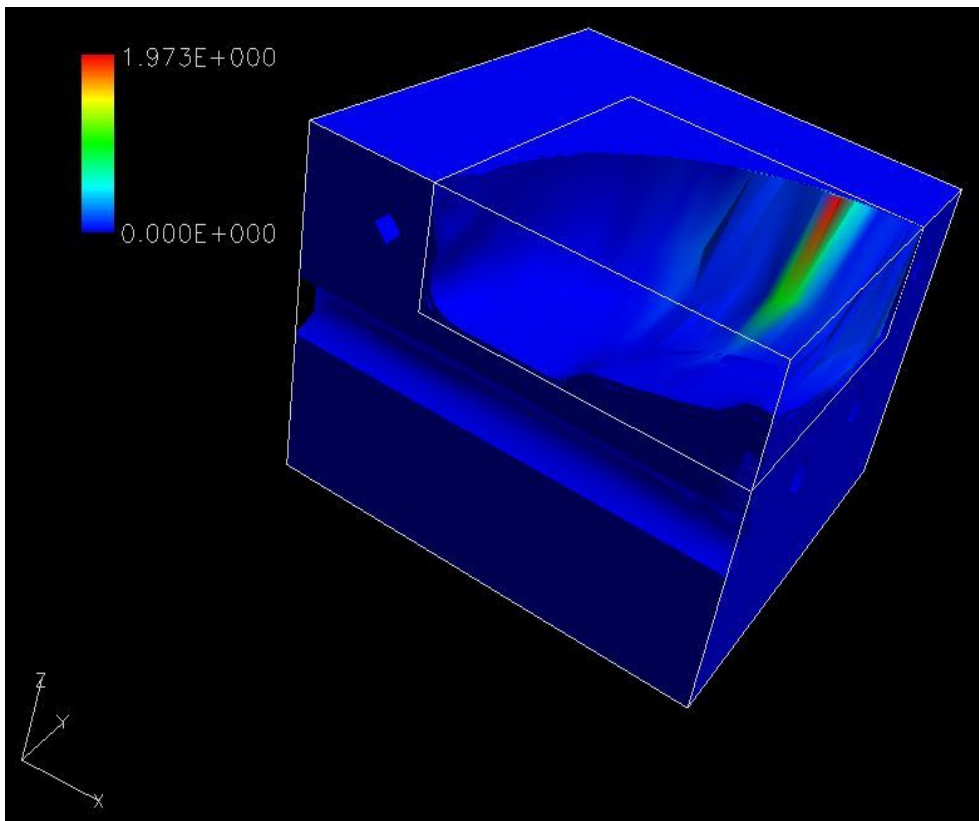


Figure 43: Variation of shear rate for Newtonian non-isothermal model with variable viscosity

The maximum value of shear strain rate is 1.97. So the assumption for the viscosity function is still good. The results for the variation of temperature and principle values of stress for this non isothermal model can be seen in Figures 44-46.

From Figures 44-46, the maximum principle stresses in the fully blown product can be observed to be $\sigma_1 = 5.25 \text{ MPa}$, $\sigma_2 = -6.38 \text{ kPa}$, and $\sigma_3 = -6.076 \text{ MPa}$. Von-Mises stress can be calculated using equation 8 to be equal to 9.813 MPa

It produces a Von-Mises strain of 0.009813 and the final product undergoes a maximum shear stress value of 11.326 MPa and shear strain value of 0.015.

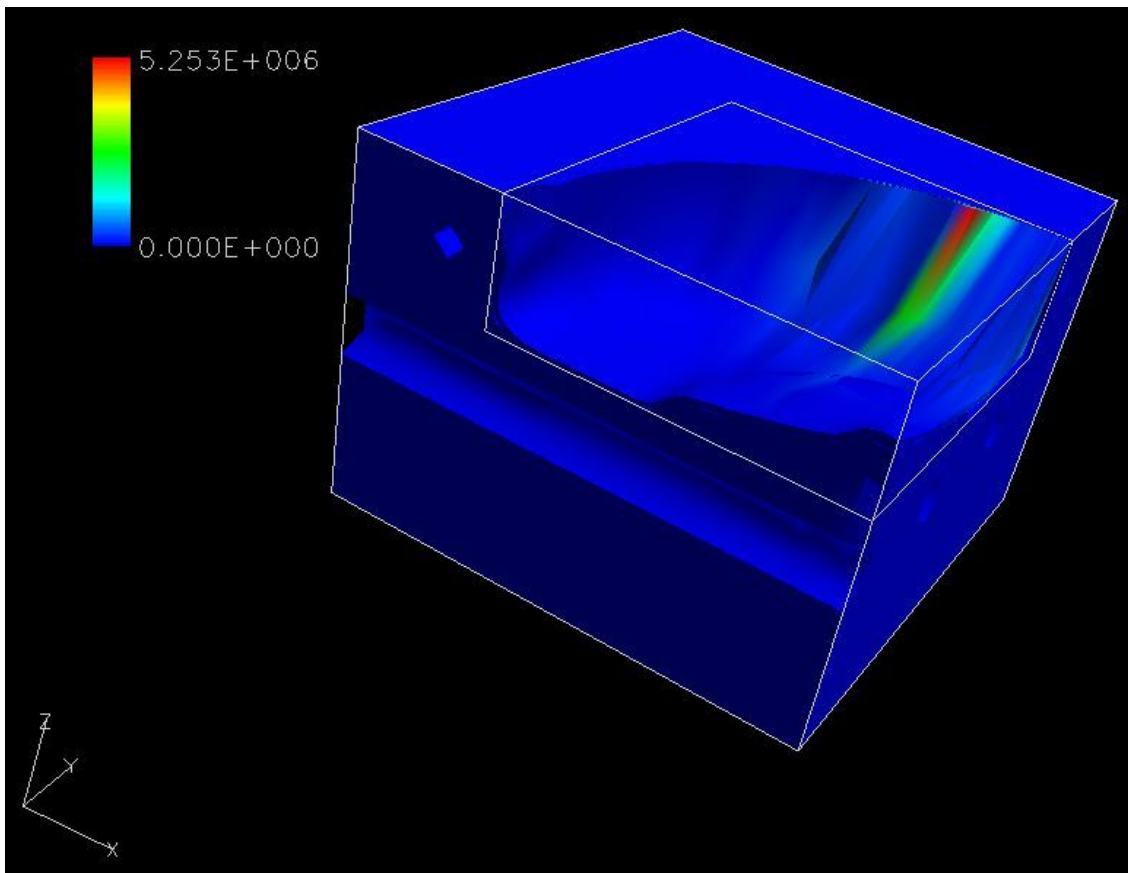


Figure 44: Variation of σ_1 for Newtonian non-isothermal model with variable viscosity

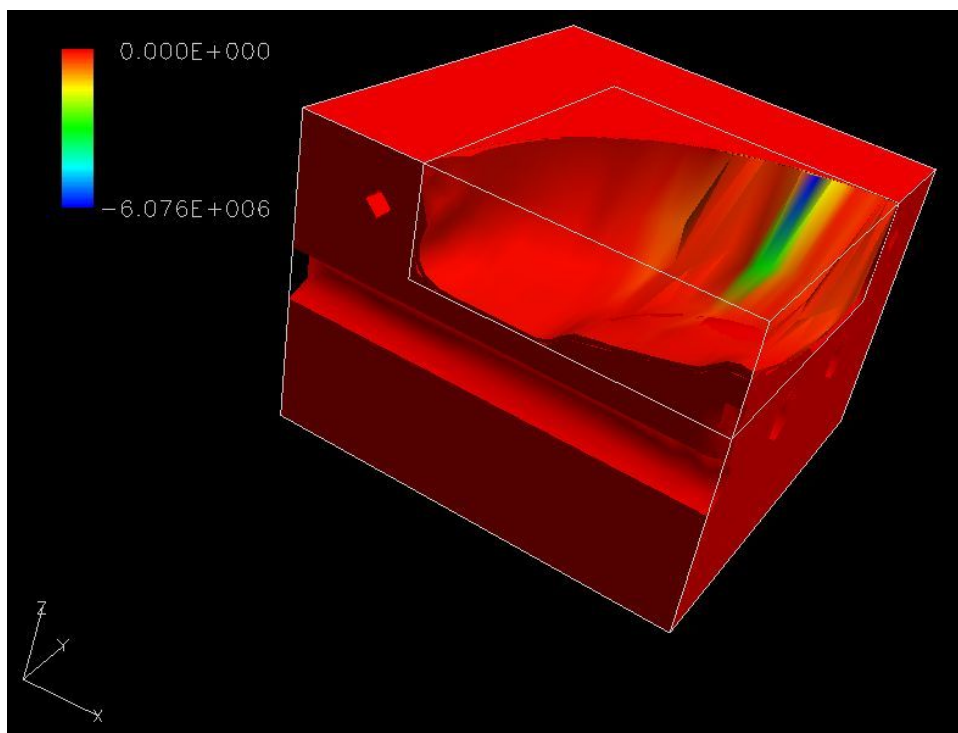


Figure 45: Variation of σ_2 for Newtonian non-isothermal model with variable viscosity

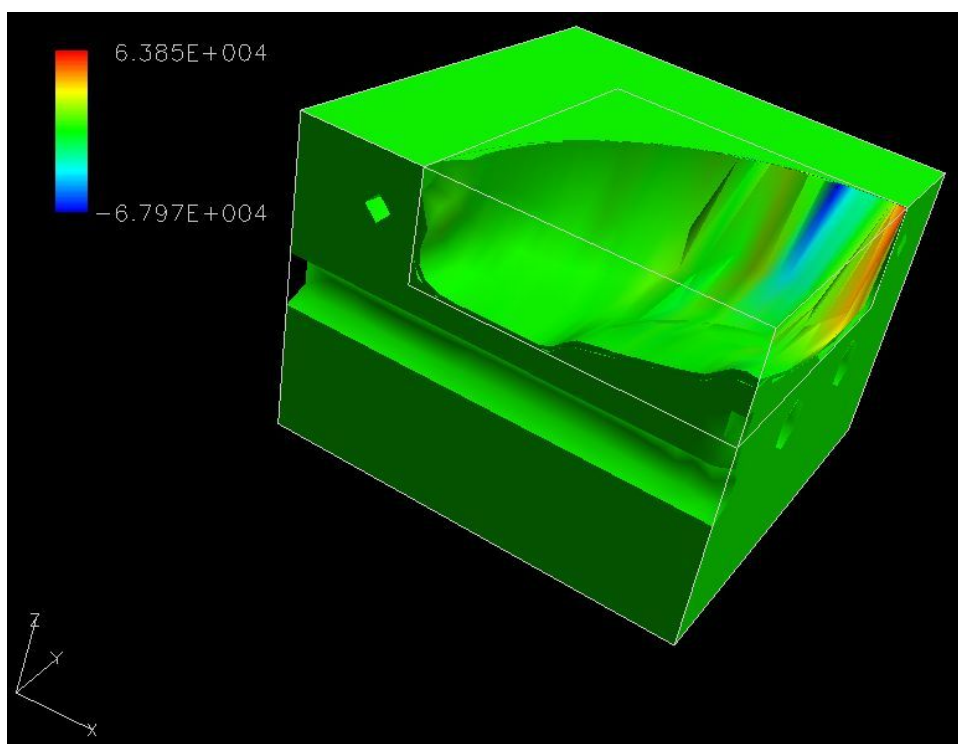


Figure 46: Variation of σ_3 for Newtonian non-isothermal model with variable viscosity

6.8.2: Integral Viscoelastic Models

For integral viscoelastic flows, the total extra-stress tensor is decomposed into two components: a viscoelastic component T_1 and a purely-viscous component T_2 . T_2 is optional and T_1 is calculated using different mathematical equations depending on the model. T_2 is optional and it is always computed using (POLYFLOW manual, version 3.12)

$$\vec{T}_2 = 2\eta_2 \vec{D} \quad (11)$$

where:

\vec{D} is the rate of deformation tensor.

\vec{T}_2 is the viscosity for the purely viscous component of the stress tensor.

η_2 is the viscosity factor for purely viscous component of stress tensor.

For HDPE, $\eta_2 = 3 \times 10^6$ Pa.s.

For an integral viscoelastic flow, T_1 is computed at time t from the following equation (POLYFLOW manual, version 3.12):

$$T_1(t) = \int_0^\infty M(s) [\Phi_1(I_1, I_2) C_t^{-1}(t-s) + \Phi_2(I_1, I_2) C_t(t-s)] ds \quad (12)$$

where:

$M(s)$ = model-specific memory (kernel) function

Φ_1 = model-specific function of the scalar invariants

Φ_2 = model-specific function of the scalar invariants

C_t = Cauchy-Green strain tensor

t = time

s = metric for time integrals (or past time measured with respect to t)

I_1 and I_2 are the scalar invariants of the Cauchy-Green strain tensor:

$$I_1 = (C_t)^{-1} \text{ and } I_2 = (C_t) \quad (13)$$

The various integral viscoelastic models are characterized by the form of the functions $M(s)$, $\Phi_1(I_1, I_2)$, and $\Phi_2(I_1, I_2)$

There are two types of integral models available in POLYFLOW: Doi-Edwards model and KBKZ model. The KBKZ model is more accurate because there is a damping function in the constitutive law equations. This model is used to model the present analysis. For KBKZ model, T_1 is calculated from the equation described below (POLYFLOW manual, version 3.12).

$$T_1 = \frac{1}{1-\theta} \int_0^\infty \sum \frac{\eta_i}{\lambda_i^2} \exp\left(\frac{-s}{\lambda_i}\right) H(I_1, I_2) [C_i^{-1}(t-s) + \theta C_i(t-s)] ds \quad (14)$$

where:

i = relaxation mode

θ = scalar parameter that controls the ratio of the normal-stress differences

H = the damping function.

λ = relaxation time.

η_i = partial viscosity.

t = time.

s = metric for time integrals (or past time measured with respect to t)

I_1 and I_2 are the scalar invariants of the Cauchy-Green strain tensor

defined in equation 11.

For the current analysis, $H = 1$, i.e. the damping is neglected for the present case. The viscosity factor for purely viscous component stress tensor, $\eta = 3 \times 10^6$ Pa.s. An eight node partial viscosity-relaxation time spectrum, Table 8, is used to describe the present model (Debaut & Rekers, 1999)

Table 8

Eight node spectrum of partial viscosities and relaxation times

Mode number, i	Relaxation time, λ_i	Partial Viscosity, η_i
1	3.331×10^{-4}	125.78
2	4.391×10^{-3}	569.07
3	2.778×10^{-2}	1842.9
4	1.682×10^{-1}	5207.5
5	1.024	12666.8
6	6.364	26366
7	4.272×10^1	52887
8	4.575×10^2	177922

KBKZ constitutive law is valid only for a thin shell model. This model can be used only for calculation of stress or temperature field on the contact surface of the mold or blown product. So this model cannot solve for the stress field in the parison or temperature field in the mold. ALGOR simulations have been used to study the temperature field in the fully blown product and the mold. Now, KBKZ model is used to

calculate the stress profile in the parison. The following two models follow KBKZ constitutive law:

(a) KBKZ Shell Model (2-D Model)

For this model, the parison is modeled as a 2-D membrane. This geometry cannot be made in the Solid Edge because if it is used to make an assembly with parison as a face, Gambit will stitch it to the mold. So the Solid Edge model of the mold is imported into Gambit and then the parison is constructed as a face (2-D membrane) in Gambit itself.

The flow is assumed to follow the constitutive law for an integral viscoelastic model. This model does not accept any volumes so the mold is modeled as the contact face and parison is also modeled as a face. No calculations can be done for the mold volume. The boundary conditions are the same as for the above described 3-D model. Parison is considered a single layer with a thickness of 5 mm. The mold contact face is meshed using 4554 triangular elements of size 0.075 and parison face is meshed using 790 triangular elements of size 0.05 (Figure 47). 2-D KBKZ model does not allow any stress or temperature postprocessor, so this model can be used to check the flow of the material with the viscoelastic constitutive law. However, because of the lack of the postprocessor, the results cannot be shown.

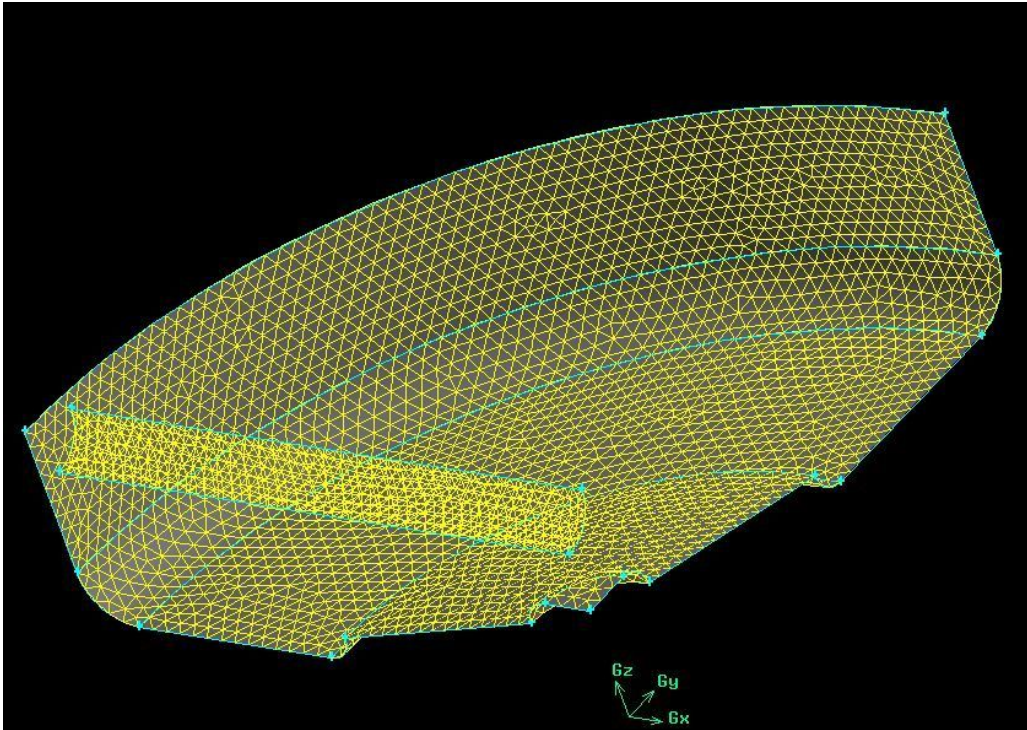


Figure 47: Meshed model – 2D KBKZ model

(b) Non-isothermal KBKZ Shell Model (3-D)

The parison and the mold are modeled as volumes in solid edge but while defining the set-up in POLYFLOW, parison is defined as a single layer membrane with a thickness equal to total parison thickness. The same eight mode spectrum, Table 8, of partial viscosities and relaxation times is used as used for the 2-D membrane model. In addition to the final principle stress values on the parison face, this model gives the temperature field in the mold volume. This model is computationally very expensive and tends to diverge for values of time increment higher than 10^{-6} . The time increment less than 10^{-6} will be impractical and it was decided to try another software to solve this problem.

CHAPTER 7: B-SIM MODEL

Since 3-D KBKZ model has convergence difficulties in POLYFLOW, it was decided to try to solve it using another software. B-SIM is a commercially used software in blow molding industry. This model was imported into a trial version of B-SIM. The preprocessor files were created and sent to Compuplast, (local B-SIM representative) for solution. Compuplast modified the preprocessor files to get the desired result. The 3-D KBKZ model was prepared by Accuform in the Czech Republic. In B-SIM simulation, the full mold was studied instead of solving one-eighth of the mold as it was done in POLYFLOW. The material properties and constants that were used for POLYFLOW simulations are also used for B-SIM simulations.

The results of the B-SIM simulation, summarized below (with permission), were obtained from Compuplast Canada Inc. (Perdikoulis, 2009). B-SIM simulation starts with two moving halves of the mold which pinches the parison and then parison starts to expand to form the wheel. It is assumed that the mold halves are 80 mm apart at the start of the simulation. They start moving towards each other with the parison placed in between. The two molds meet each other and pinch the parison in 1 second. The air pressure increases linearly in 5 seconds to a maximum constant value of 400 kPa. The diameter of the parison for B-SIM simulation is taken to be 60 mm with a mean thickness of 5 mm. The total time of the simulation is 9 seconds.

The different stages of expansion during the cycle are shown in Figure 48.

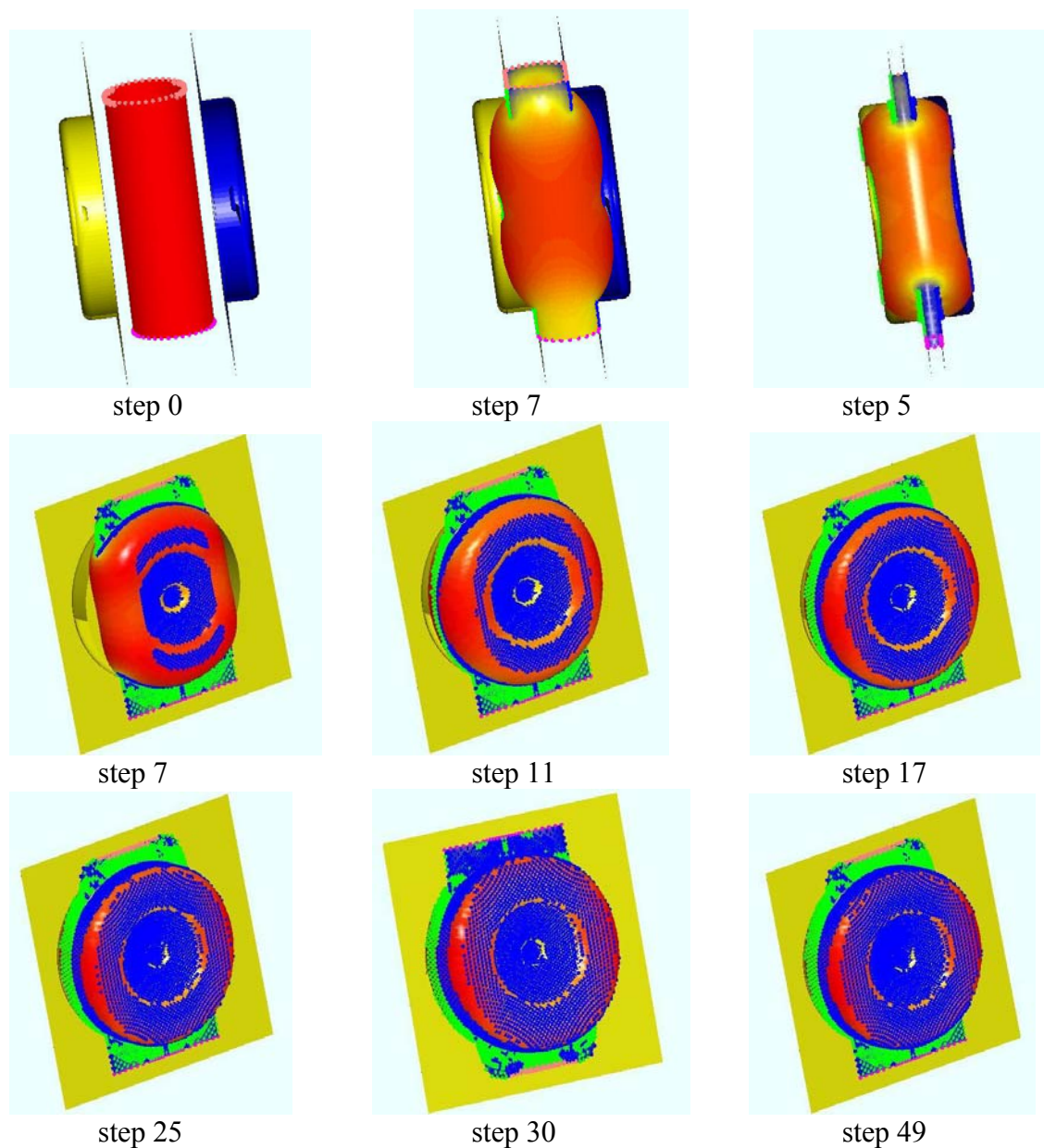


Figure 48: Stages of expanding parison (Perdikoulis, 2009)

The initial thickness of the parison is 5 mm. After complete inflation, the thickness of the blown product varies from 1.1 mm to 5 mm. The thickness variation in the blown wheel is shown in Figure 49.

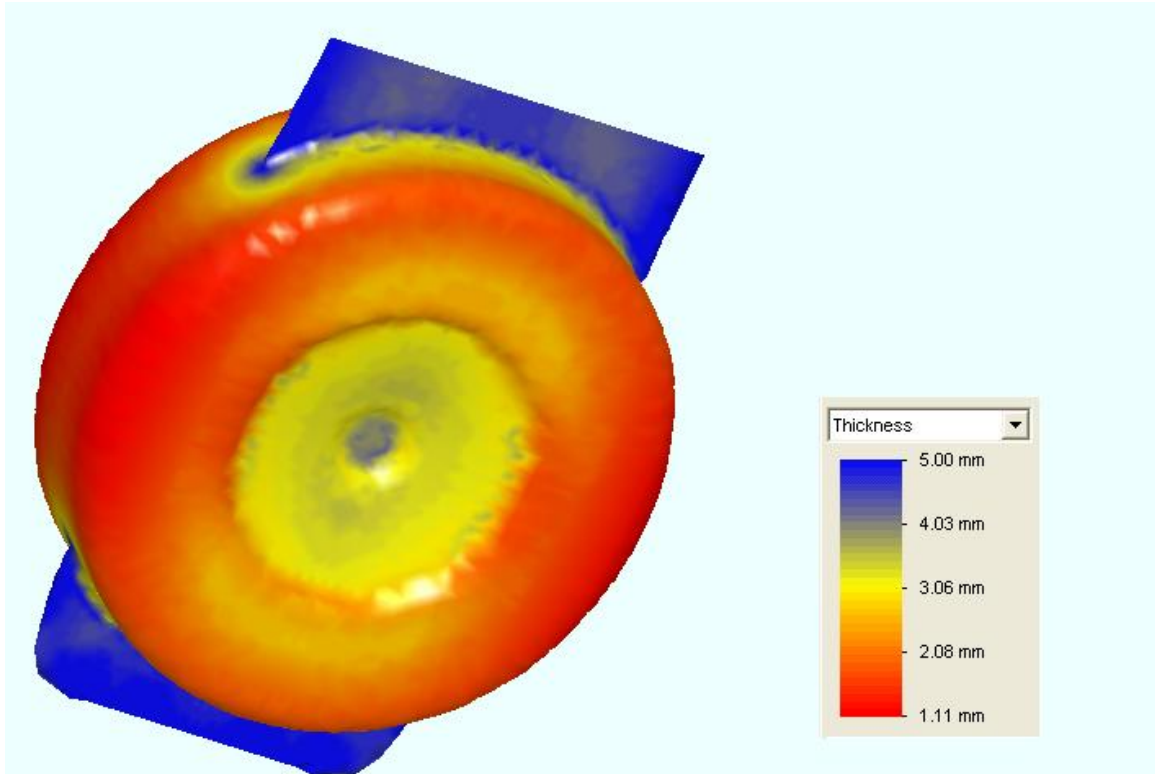


Figure 49: Thickness profile in the blow molded wheel (Perdikoulis, 2009)

The maximum thickness of the blow molded wheel lies in the central region. This part is the closest to the parison. Actually this part of parison touches the mold before closing of the mold. So there is no expansion in this region and thickness of the final product remains 5 mm which is equal to the initial thickness of the parison.

The Von-Mises stress for the final expanded parison varies from 0 MPa to 4 MPa. The variation of Von-Mises stress is shown in Figure 50.

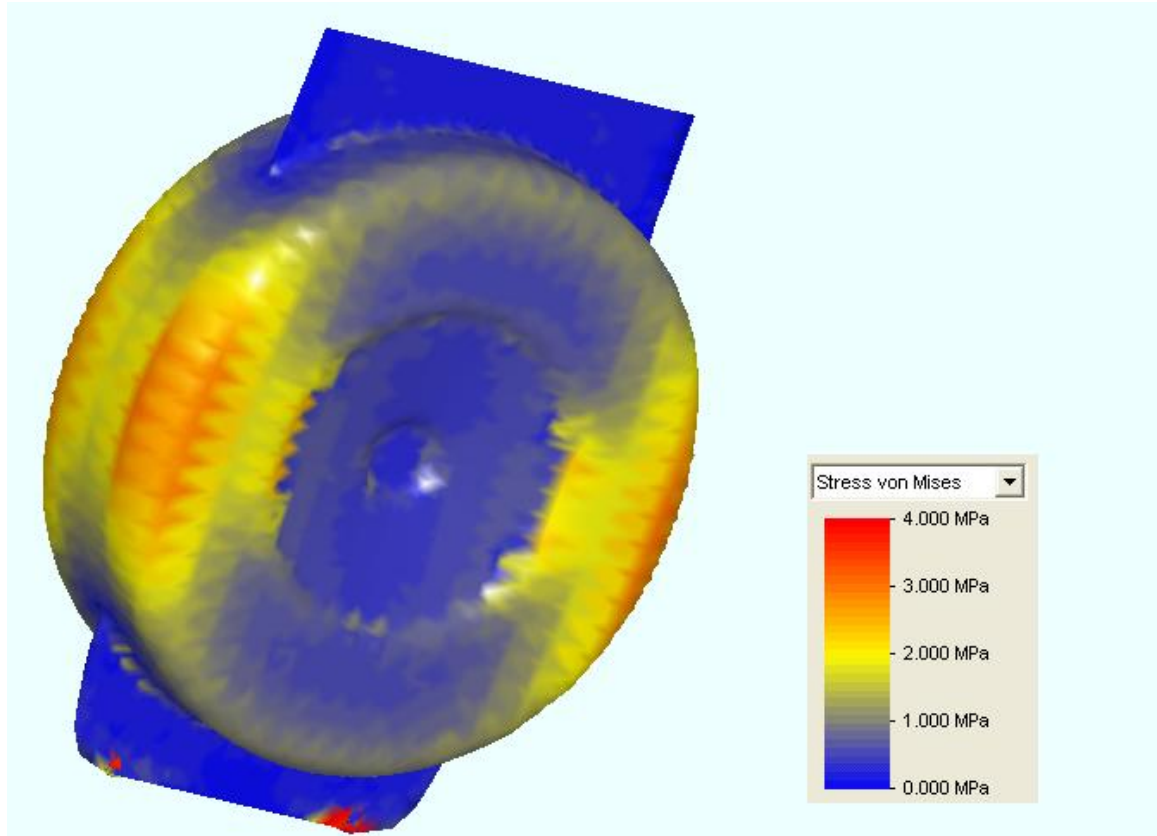


Figure 50: Von-Mises stress profile in the final blow molded wheel (Perdikoulis, 2009)

The maximum Von-Mises stress is present in the region which is farthest from the initial position of the parison. This region undergoes maximum expansion which makes it the thinnest region of the blow product and the Von-Mises stress is also the maximum due to the maximum elongation.

CHAPTER 8: DISCUSSION AND CONCLUSIONS

The design of a nanocomposite blow mold has been carried out using numerical solution methods available in several commercial engineering software packages. The thermal design process for a nanocomposite mold for a polymer wheel using the ALGOR software produced a design with one loop of cooling tube around the mold cavity and five straight cooling channels under the mold. The maximum temperature of the polymer layer for this mold at the steady cyclic state is was found to be 103 °C which is a safe ejection temperature. The cycle time for this design was calculated to be 80 seconds, which is approximately four times the typical value for a metal mold. Therefore, it can be concluded that the nanocomposite mold will increase the cycle time and reduce the production rate.

The thermal design was followed by a stress analysis of the polymer wheel during the blow molding process. This analysis was carried out by using POLYFLOW and B-SIM software. In POLYFLOW, several different models were examined, including a Newtonian non-isothermal flow with the viscous flow modeled by the modified Cross law. This approach is expected to provide a good estimate of the stress history since the shear rates are small. However, it was determined that the flow models in POLYFLOW were very general and difficult to apply for the blow molding process. Therefore, an arrangement was made to have a simulation carried out using B-SIM, a software developed by Compuplast Canada Inc. specifically for the blow molding process. The problem was solved in B-SIM by using an integral viscoelastic model (KBKZ model), which is known to be an accurate model for this process.

The maximum von-Mises stress in the model varies from 1.8 MPa to 9.8 MPa depending on the constitutive law used. These values are small compared to the tensile strength of the polymer. Therefore, the product is expected to be free of structural defects, such as tears or holes. As already discussed, the life of the nanocomposite blow mold is expected to be very low as compared to its metal counterparts. Therefore, it is recommended only for short runs or prototypes.

For a successful process cycle, the parison dimension had to be made significantly bigger in the B-SIM simulation. The thickness of the final product, as calculated in the simulation, ranged from 1.1 mm to 5 mm. The thickness variation will produce a change in the cycle time, since the cooling time of the polymer also increases with thickness. Therefore, several iterations of this design process are required to produce a final design. If the B-SIM software becomes available to Ohio University, further design iterations should be carried out.

CHAPTER 10: FUTURE WORK

Blow molding is a complex process because of the thermal and stress fields that arise when a non-Newtonian fluid (polymer melt) undergoes solidification during deformation. Thermal analysis of the process was done using ALGOR, which does not have any mathematical model for a non-Newtonian fluid. On the other hand, the stress analysis has been done using B-SIM software. B-SIM uses only the contact surface of the mold, so it is not able to calculate the temperature field inside the mold. Consequently, the stress and temperature fields for the blow mold in this project were calculated separately by two different software packages. For a more accurate and efficient simulation, the process should be analyzed as a coupled thermo-mechanical problem. Therefore the numerical simulation of this process requires special integration of different software. This is recommended as a future goal for this project.

The process simulation carried out in this study did not examine the effect of residual stresses after the polymer part is ejected from the mold. This should be done by using the residual stresses to predict the warping or deformation that may occur in the final product. The mold design can then be refined further to improve the quality of the product.

The nanocomposite blow mold may become a useful alternative to metal molds for making prototypes; however, the number of parts that can be made in the mold is not known. It will be highly beneficial to analyze the life span of the nanocomposite mold by studying the wear and tear of the mold in actual production.

The cycle time of the process came out to be 80 seconds which is approximately four times the normal cycle time with a metal mold. In practice, the true cycle time may be even higher because of non-uniform thickness of the part. Therefore, more work should be done to increase the cooling efficiency of the mold to bring down the cycle time. It can also be done by considering enhancement of the internal cooling.

REFERENCES

- Alam, M. K., Klein, P., & Garg, D. (2009). Simulation of thermal transport in a nanocomposite blow mold, 2009 ASME Summer Heat Transfer Conference Proceedings, Paper no. HT2009-88265.
- Ajayan, P. M., Redlich, P., & Ruhle, M. (1997). Structure of nanotube-based nanocomposites. *Journal of Microscopy*, 185, 275-282.
- Blow Molding. (2006). Engineers Handbook. Retrieved October 12, 2008, from <http://www.engineershandbook.com/MfgMethods/blowmolding.htm>
- Chereources (2008). Retrieved October 22, 2008, from <http://www.cheresources.com/convection.shtml>
- Debaut, B., & Rekers, G. (1999). Influence of HDPE grade on the blow moulding of a bottle: A numerical investigation. *SPE/ANTEC Proceedings*, 1, 1993-1998.
- Fitzer, E., & Manocha, L. M. (1998). *Carbon reinforcements and carbon/carbon composites*. Berlin, Heidelberg, Germany: Springer-Verlag.
- Gong, Q., Li, Z., Zhang, Z., Wu, B., Zhou, X., Huang, Q., Z., & Liang, J. (2006). Tribological properties of carbon nanotube-doped carbon/carbon composites. *Tribology International*, 39, 937-944.
- Gong, Q., Li, Z., Bai, X., Li, D., Zhao, Y., & Liang, J. (2004). Thermal properties of aligned carbon nanotube/carbon nanocomposites. *Materials Science and Engineering*, A(384), 209-214.

- Gong, Q., Li, Z., Li, D., Bai, X., & Liang, J. (2004). Fabrication and structure: A study of aligned carbon nanotube/carbon nanocomposites. *Solid State Communications*, *131*, 399-404.
- Gong, Q., Li, Z., Zhou, X., Wu, J., Wang, Y., & Jiang, Li. (2005). Synthesis and characterization of in situ grown carbon nanofiber/nanotube reinforced carbon/carbon composites. *Letters to the Editor / Carbon*, *43*, 2397-2429.
- Han, K., & Rice, B. (2008). Mold Design and Manufacturing Using Nanocomposite Materials. *SAMPE Journal*, *44*(1), 20-27.
- Perdikoulis, J. (2009). B-SIM contact person, Compuplast Canada Inc., Personal communication.
- POLYFLOW Manual, Version 3.12.
- Rosato, D. V., Rosato, A. V., & Dimattia, D. P. (2004). *Blow Molding Handbook*. Munich, Germany: Hanser Publications.
- Strong, B., Blow Molding (2008). Retrieved November 20, 2008, from http://www.et.byu.edu/groups/mfg355/pages/lectures/powerpoint_ppt/13%20blow%20molding.ppt
- Vinogradov, G. V., & Malkin, A. Y. (1966). Rheological Properties of Polymer Melts. *Journal of Polymer Science: Part A-2*, *4*, 135-154.